FYS 3610
University of Oslo, 2009

OZONE

AND

UV-RADIATION

Preface

This compendium is a part of the course FYS3610 – Space Physics. It reflects ongoing atmospheric research activities at Plasma and space Physics (Department of Physics, University of Oslo). Figures and text are gathered from various sources, but many ideas are from the Norwegian book "Ozonlag, UV-stråling and Helse" (Henriksen and Svendby, 1997, ISBN 82-992073-9-8).

Blindern, August 2009

Content

Chapter 1: Radiation from the sun …… 5

Chapter 2: What is ozone? ……..….. 16

Chapter 3: Ozone measurement techniques ……. 22

Chapter 4: Ozone measurements and trends …… 36

Chapter 5: Ozone formation and destruction ……..…. 46

Chapter 6: UV-radiation through the atmosphere ……..... 58

Chapter 7: Radiative transfer in the atmosphere ……...……...… 69

Exercises ……..…… 72

References ……..….. 73

Chapter 1

Radiation from the sun

1.1. Introduction

Ozone is one out of many gases in the stratosphere. Although the concentration of ozone is relatively small it plays an important role for life on Earth due to its ability to absorb ultraviolet radiation (UV) from the sun. In the course of the last 20 years we have often heard about "*the depletion of the ozone layer"* and the co-called "*ozone hole"*, which have been considered as a threat to our health and environment.

Every day we release a number of gases that pollute the atmosphere and some of these gases may also have a negative influence on the ozone layer. The ozone destroying gases are in the first place halogens, i.e. compounds containing chlorine (Cl) or bromine (Br). These gases are also effective "*greenhouse gases".* Fortunately, international agreements (the Montreal Protocol) have been signed to reduce the release of ozone destroying substances and the restrictions seem give positive results.

In the next chapters we will learn about the ozone layer, how ozone is formed and destroyed. We will see how ozone is measured with ground based instruments and from satellites. Furthermore, we will describe the radiation passing through the atmosphere and ozone layer and discuss how it influences the UV-radiation reaching the ground. We live in an UV-environment that varies with latitude, cloud formation and time of the year.

In order to discuss the ozone layer and the effect of UV-radiation it is necessary to have some knowledge about the electromagnetic radiation from the sun. The next chapters give an introduction to solar radiation and how it is absorbed by the ozone layer, but first we start with a brief description of the atmosphere.

1.2. Vertical structure of the atmosphere

The atmosphere surrounding the Earth is divided into four spherical strata separated by narrow transition zones (see Figure 1.1). The upper boundary where gases disperse into space is at an altitude of approximately 1000 km above sea level. Atmospheric layers are characterized by differences in chemical composition that produce variations in temperature. In fact, the variation of average temperature profile with altitude is the basis for distinguishing the layers of the atmosphere. The four regions of the atmosphere are

the troposphere, the stratosphere, the mesosphere, and the thermosphere. The two lowest strata are of main interest when studying the ozone layer.

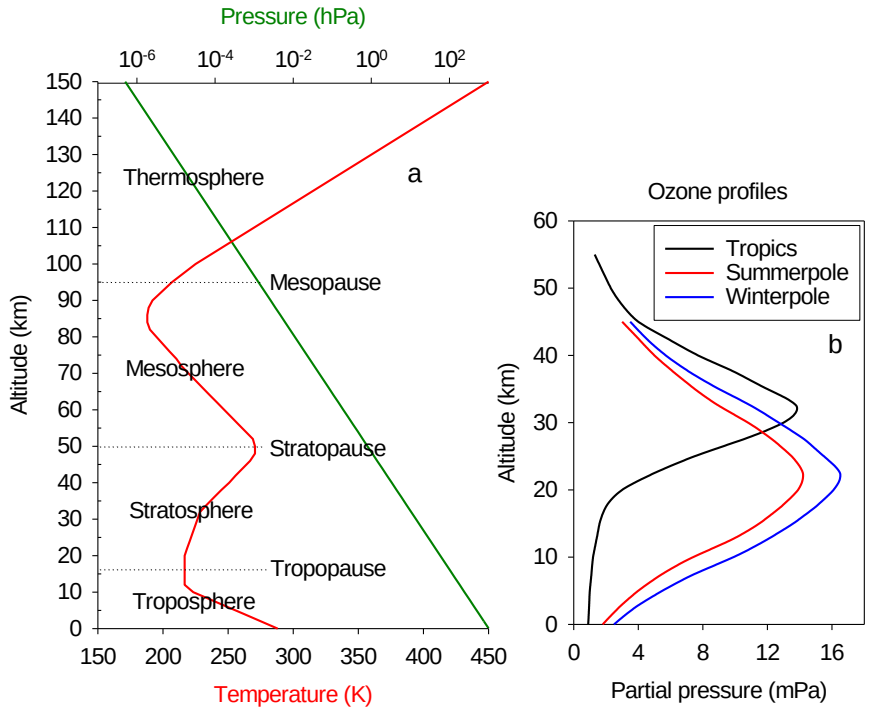

Figure 1.1*: Atmospheric altitude profiles: a) Temperature (red line) and atmospheric pressure (green line), b) Ozone distribution in the tropics (black line) and at high latitudes during summer (red line) and winter (blue line) [Stordal and Hov, 1993].*

Troposphere. The troposphere is the atmospheric layer closest to the Earth's surface and contains about 80% of the atmospheric mass. It is characterized by high air density and an average vertical temperature decrease of 6-7 K per km. Essentially all weather phenomena occur within the troposphere, although turbulence may extend into the lower part of the stratosphere. A narrow zone called the tropopause separates the troposphere from the next layer. The altitude of the tropopause varies with latitude and season and can range from 8-10 km at the poles to 16-18 km at the equator. Within this zone the air temperature is relatively constant.

Stratosphere. The stratosphere extends from the tropopause to the stratopause (~45 to 55 km above the surface) and is the second major stratum of the atmosphere. The air temperature in the stratosphere remains relatively constant up to an altitude of 20-25 km. It then increases gradually, reaching about 270 K at the lower boundary of the stratopause, a temperature not much lower than the average 288 K at the Earth's surface. Because the air temperature in the stratosphere increases with altitude, it does not cause convection and has a stabilizing effect on atmospheric conditions in the region. Absorption of solar ultraviolet radiation by ozone is the main reason for the stratospheric heating.

Mesosphere. The mesosphere, a layer extending from approximately 50 km to 80 km, is characterized by decreasing temperatures. At an altitude of about 80 km the temperature reaches 190-180 K, which is the coldest point in the atmosphere. In this region, concentrations of ozone and water vapour are negligible.

Thermosphere. The thermosphere is located above the mesosphere, separated by the mesopause transition layer. The temperature in the thermosphere generally increases with altitude due to the absorption of intense short wave solar radiation by the limited amount of remaining molecular oxygen and nitrogen. At this extreme altitude gas molecules are widely separated. The actual temperature in the thermosphere can reach as high as 2000ºC! This temperature, however, cannot be measured by a conventional thermometer (it would read below 0ºC) because there are not enough particles to strike a thermometer to heat it. The *ionosphere* is a shell of electrons and electrically charged atoms and molecules that mainly is located in the thermosphere. The charged molecules/atoms (ions) are formed by high energy solar radiation.

The temperature in the lower 100 km of the atmosphere varies by less than a factor 2, while the pressure changes by six orders of magnitude (see the green line in Figure 1.1). If the temperature is taken to be approximately constant, the pressure at height (z) can roughly be described by the exponential function

$$p(z) = p(0) \cdot e^{-z/H} \qquad (1.1)$$

where $H=RT/M_{air}g$ is called the **scale height** (characteristic length scale for decrease of pressure with height), R is the Molar gas constant (8.314 J/mol K), T is temperature in Kelvin, M_{air} is molecular weight of air (28.97 g/mol), g is acceleration due to gravity, and $p(0)$ is the surface pressure. The SI pressure unit is hectopascal (hPa). The relationship between different pressure units is:

$$1 \text{ atm} = 1.01325 \cdot 10^5 \text{ Pa} = 1013.25 \text{ mbar} = 1013.25 \text{ hPa}$$

1.3. Atmospheric composition

The most abundant gases found in the Earth's lower atmosphere are listed in Table 1.1. Of the gases listed, nitrogen, oxygen, water vapour, carbon dioxide, methane, nitrous oxide, and ozone are extremely important to the Earth's biosphere.

The table indicates that nitrogen and oxygen are the main components of the atmosphere by volume. Together these two gases make up approximately 99% of the dry atmosphere. Both of these gases have very important associations with life. Nitrogen acts as important nutrition for plant growth. The gas is removed from the atmosphere and deposited at the Earth's surface mainly by specialized nitrogen fixing bacteria. Also lightning can cause oxygen and nitrogen to combine and form reactive nitrogen oxides.

Table 1.1: Average composition of the atmosphere up to an altitude of 25 km.

Gas Name	Chemical Formula	Percent Volume
Nitrogen	N_2	78.08%
Oxygen	O_2	20.95%
*Water	H_2O	0 to 4%
Argon	Ar	0.93%
*Carbon dioxide	CO_2	0.0360%
Neon	Ne	0.0018%
Helium	He	0.0005%
*Methane	CH_4	0.00017%
Hydrogen	H_2	0.00005%
*Nitrous oxide	N_2O	0.00003%
*Ozone	O_3	0.000004%
*Halocarbons	$CFCl_3$,CF_2Cl_2, …	0.00000008%

*variable gases

Oxygen is mainly exchanged between the atmosphere and life through the processes of photosynthesis and respiration. Photosynthesis produces oxygen when carbon dioxide and water are chemically converted into glucose with the help of sunlight.

The next most abundant gas in the table is water vapour. Water vapour varies in concentration in the atmosphere both spatially and temporally. The highest concentrations of water vapour are found near equator over the oceans and tropical rain forests. Cold polar areas and subtropical continental deserts are locations where the water vapour can approach zero percent. Water vapour has several important functional roles on our planet:

- It redistributes heat energy through latent heat energy exchange (evaporation and condensation).
- The condensation of water vapor creates precipitation that falls to the Earth's surface providing fresh water for plants and animals.
- It helps warm the Earth's atmosphere through the greenhouse effect.

The fifth most abundant gas in the atmosphere is carbon dioxide. The volume of this gas has increased from about 315 ppb to about 385 ppb over the last 50 years! This increase is primarily due to human activities such as combustion of fossil fuels, deforestation, and other forms of land-use change. Carbon dioxide is also exchanged between the atmosphere and life through the processes of photosynthesis and respiration.

The ozone gas can be found in two different regions of the Earth's atmosphere. The majority of the ozone (about 97%) is concentrated in the stratosphere at an altitude of 15 to 55 km. This stratospheric ozone provides an important service to life on the Earth as it absorbs harmful ultraviolet radiation.

High ozone concentrations can also be found at the Earth's surface, especially in and around cities. Most of this ozone is created as a byproduct of human-created photochemical smog. This build up of ozone is toxic to organisms living at the Earth's surface.

The last row in Table 1.1 lists a group of compound which plays an essential role for the ozone layer and the climate on Earth: the halocarbons. They consist of one or more carbon atoms which are linked by covalent bonds with one or more halogen atoms: fluorine, chlorine, bromine or iodine. The formation and destruction of ozone and the role of halocarbons will be described in detail in chapter 2 and 5.

1.4. Radiation from the sun

The sun plays an essential role in the formation and destruction of ozone. Figure 1.2 illustrates the solar spectrum, where the solar intensity is given as a function of wavelength at the top of the atmosphere and at the Earth's surface. The wavelength is usually given in nanometer (nm, 10^{-9} m) and the intensity in W/m^2. At the top of the atmosphere the solar energy is approximately 1367 W/m^2 (the "*The solar constant"*).

From outer space the Earth looks like a flat circular area with the size πR^2. The radiation is distributed over the whole globe with the surface $4\pi R^2$, but approximately 30% of the radiation is absorbed or reflected back to space. The radiation that finally reaches the Earth's surface is in average 235 W/m^2. Can you derive this number? In exercise 2 on page 72 you are asked to calculate the average energy reaching the ground.

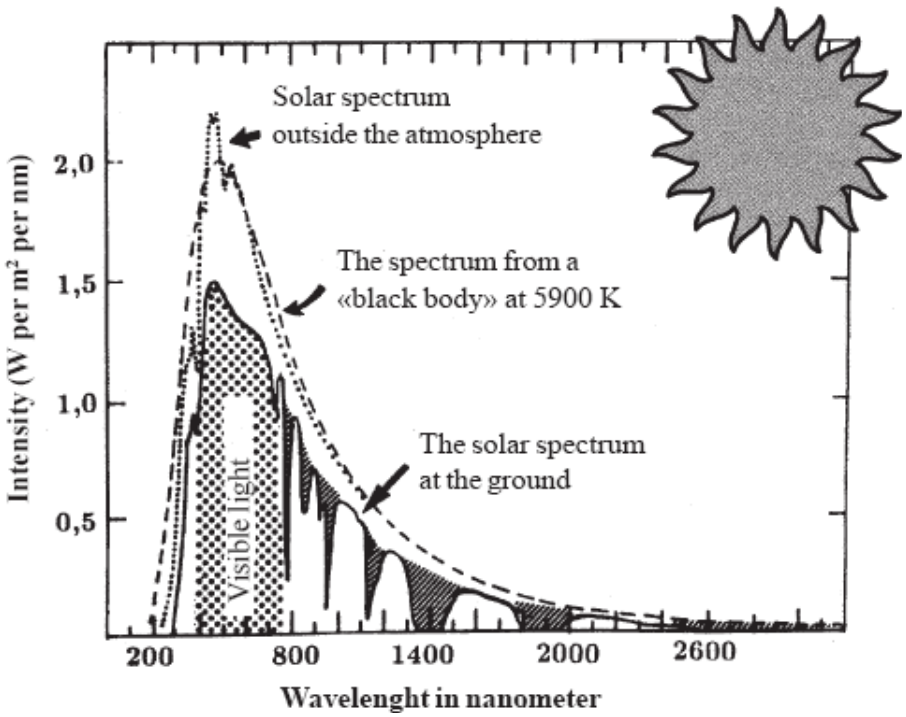

Figure 1.2: *The solar spectrum at the top of the atmosphere (dotted) and at the Earth's surface (solid line). The dashed curve represents the spectrum from a "black body" (see next side) with a temperature of 5900 K. The spectrum at the surface of the Earth has a number of shaded areas, caused by absorption from different gases in the atmosphere. Ozone absorbs in the UV-region as well as in the visible region. Water and CO_2 mainly absorb at longer wavelengths.*

1.5. Electromagnetic radiation

The solar spectrum in Figure 1.2 indicates that the surface solar radiation range from approximately 300 nm to about 2500 nm. Radiation with wavelengths below 400 nm is called UV (Ultra Violet), whereas radiation with wavelength above approximately 800 nm is called infrared.

The human eye can register radiation with wavelengths from 400 nm to 800 nm. The retina contains certain molecules (chromophores) that absorb radiation. This absorption will produce nerve pulses which travel to the brain and cause vision.

The electromagnetic spectrum includes radiation known as e.g. radio waves, microwaves, visible light, UV and X-rays. In the UV and visible range the wavelength is normally used to characterize the radiation. In the X-ray region we usually characterize the radiation by the photon energy (eV), but in the region for TV and radio waves the radiation is characterized by the frequency.

Black bodies

The "*black body*" model system can be used to describe the radiation from the sun as well as from the Earth. This is an object that has the ability to absorb all radiation. In reality such bodies hardly exist, but a small hole in a hollow black carbon sphere comes quite close to the definition.

A black body emits radiation depending upon its temperature. Three physical laws can describe the radiation:

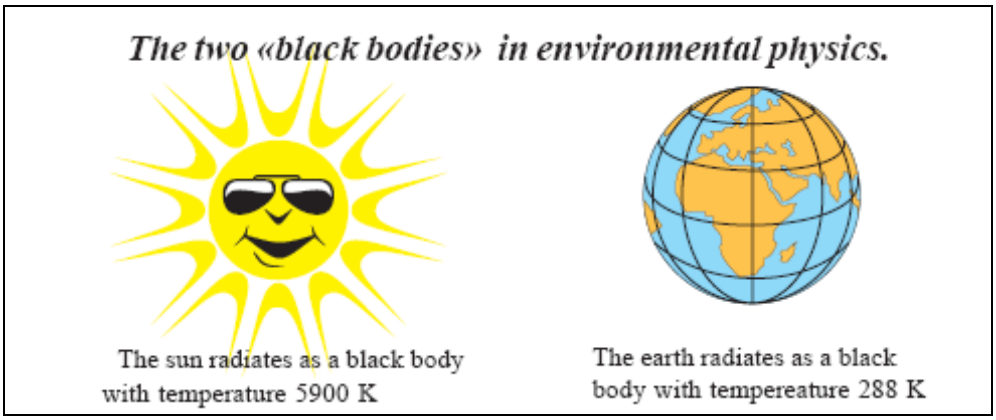

1. **Stefan-Boltzmann's law** determines the total heat energy radiated from a block body:

$$\mathbf{E = \sigma T^4}$$

T is the temperature (in Kelvin) and $\sigma = 5.6693 \cdot 10^{-8}$ W/m^2 K^{-4} is Stefan-Boltzmanns constant.

2. **Planck's law** gives the spectrum of the emitted radiation, i.e. the energy as a function of wavelength. An example is given by the dashed curve in Figure 1.2.

3. **Wien's law** describes the relationship between the temperature of the black body and the wavelength λ of maximum intensity. The relationship is given by:

$$\mathbf{\lambda T = 2.88 \cdot 10^{-3}}\ \text{mK}$$

Table 1.2: The regions of UV-radiation

320 - 400 nm UVA 280 - 320 nm UVB 200 - 280 nm UVC 100 - 200 nm Vacuum UV

The UV-region is for practical purposes divided into 4 regions (see Table 1.2). The short wavelength region 100 - 200 nm is usually called vacuum-UV since radiation in this region is absorbed very easily and can only be studied in vacuum. UVC (200 – 280 nm) is absorbed high up in the atmosphere, whereas UVB (280 – 320 nm) and UVA (320 – 400 nm) can reach the ground. Quartz absorbs radiation with wavelengths below 200 nm, whereas ordinary window pane glass absorbs everything below 300 nm.

The Earth can be characterized as a "*black body"* with an average temperature of 15°C (288 K) which emits radiation. The spectral form is given by Planck's law, whereas the wavelength for maximum intensity can be described by Wien's law, i.e. it has a maximum at approximately 10 000 nm (10 micrometer).

1.6. What is UV-radiation?

UV-radiation, like the rest of the electromagnetic radiation, can be described either as waves or particles (photons).

The duality of radiation implies that we can describe a number of different phenomena in a simple way. For example, interference can easily be described when we assume that the light is a wave, whereas other phenomena such as the photoelectric effect make it necessary to describe light as photons.

The energy of a photon (E) is given by:

$$E = h\nu$$

where $h = 6.62 \cdot 10^{-34}$ Js is Planck's constant. The relationship between frequency ν and wavelength λ is given by

$$\lambda\nu = c$$

where c is the velocity of light in vacuum ($3.0 \cdot 10^8$ m/s). Consequently, the energy can be written as:

$$E = \frac{hc}{\lambda} \tag{1.2}$$

The energy of a photon is usually given in "*electron volt"* (eV). The unit is defined as the energy attained by an electron accelerated through a voltage gap of 1 volt. The relationship between electron volt and joule is:

$$1 \text{ eV} = 1.6 \cdot 10^{-19} \text{ J}$$

If the constants *h* and *c* are used in the energy equation (1.2) we have the following formula for photon energy:

$$\boxed{E = \frac{1240}{\lambda}} \tag{1.3}$$

Here E is given in eV and λ is in nm. Based on this expression we get the relationship between photon energy and wavelength as described in Table 1.3.

Table 1.3: The relationship between wavelength and energy for certain spectral lines

WAVELENGTH (in nm)	NAME	ENERGY (in eV)
121.57	Lymann λ	10.20
200	Vacuum UV	6.20
242.4	Splits oxygen	5.115
254	UVC (Hg-lamp)	4.88
280-320	UVB	4.43-3.87
320-400	UVA	3.87-3.10
400-800	Visible light	3.10-1.55
1240	Infrared	1.0
10 000	Radiation from Earth	0.124

1.7. Absorption of UV-radiation

The solar radiation will partly be absorbed in the atmosphere. The absorption is determined by the composition of atoms and molecules.

UV-radiation with the shortest wavelengths is absorbed by oxygen far out in the atmosphere (70 - 80 km above sea level). Next, a significant fraction of the radiation in the UVC and UVB regions is absorbed by the **ozone layer**. As seen from Figure 1.1b the majority of ozone at high latitudes is located 15 to 25 km above the ground.

The absorption of radiation can be described by Lambert-Beers law: When a parallel *monochromatic* beam penetrates a medium (a gas, liquid or a solid compound), the intensity decreases according to an exponential law:

$$I_x = I_0 e^{-\alpha x}$$

I_0 is the intensity when the radiation hits the absorbing compound (i.e. when $x = 0$), I_x is the intensity at depth x, and α is a constant called the "*absorption coefficient*". The absorption depends on the wavelength of radiation and the constant, α, which is given as the absorption *per unit length* (it can also be expressed *per mass unit* or *per molecule*).

The absorption spectrum describes how the absorption coefficient α varies with wavelength.

The absorption spectrum varies from one compound to another. Figure 1.3 shows the absorption spectrum for ozone. Note that the ordinate axis is given in logarithmic units to visualize the differences in absorption for various wavelengths. The absorption is much larger in UVB and UVC than in UVA. Ozone also absorbs in parts of the visible spectrum. Since the photosynthesis depends on visible light, the thickness of the ozone layer might influence vegetation and photosynthesis.

Figure 1.3 shows that the absorption is weak in the UVA region. This implies that all processes that depend on UVA-radiation are more or less independent of the thickness of the ozone layer.

Ozone also absorbs in the infrared region around 9.6 μm (not shown in Figure 1.3). Due to this IR absorption ozone is an important greenhouse gas. A further description of the relationship between ozone and the greenhouse effect will not be discussed in this compendium.

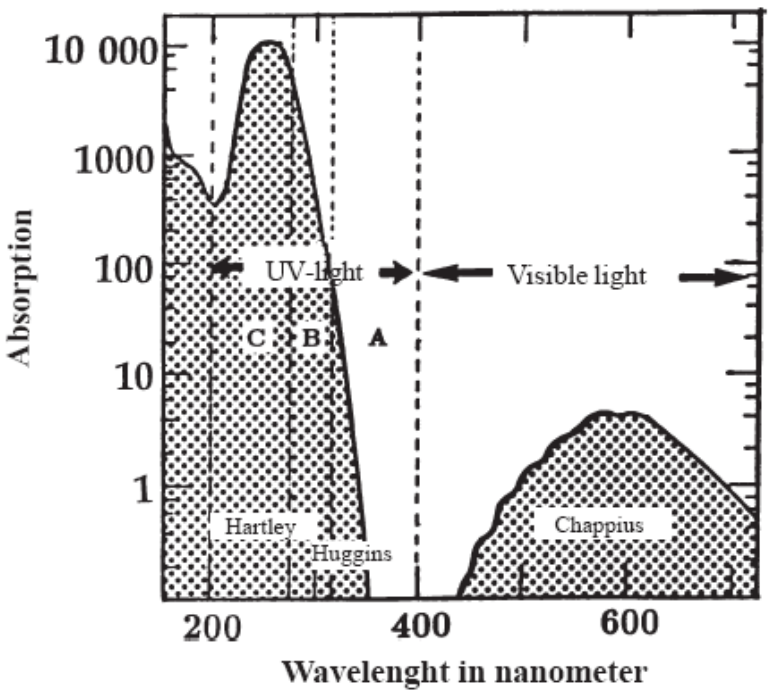

Figure 1.3: *The absorption spectrum of ozone in the wavelength region 180 - 720 nm. Different regions of the absorption spectrum have been given names after scientists working in the field. The region from 200 to 300 nm is called the Hartley-band. The region from 300 to 350 nm is called the Huggins-band and in the visible region we have the Chappius-band.*

G.M.B. Dobson (1889 - 1976) was the great pioneer in the ozone field. Dobson constructed instruments for ozone measurements, in the first place the famous Dobson spectrometer. In order to honour Dobson and his work the unit for the thickness of the ozone layer is named after him: Dobson unit (DU).

Chapter 2

What is ozone?

2.1. The ozone molecule

Ozone is an invisible, poisonous gas consisting of three oxygen atoms with the chemical formula O_3.

Oxygen exists in three different forms: atomic oxygen (O) which mainly are found high up in the atmosphere, ordinary molecular oxygen (O_2) and ozone (O_3).

The structure of the ozone molecule is illustrated in Figure 2.1.

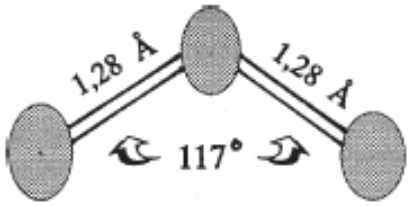

Figure 2.1: *The structure of ozone. The three oxygen atoms form a plane where the angle between the two chemical bonds is 117°. The bond lengths are 1.28 A or 0.128 nm.*

For interested readers

2.2. The structure of the ozone molecule

The structure of the ozone molecule is shown in Figure 2.1. The orbits of the three oxygen atoms are sp^2 – hybridized, which theoretically would give a molecule with an angle of 120° between the two bonds. This is in relatively good agreement with the experimental value of 117°. The molecule has four π-electrons, which give the two bonds a significant double-bond character. The bond-length of 1.28 A is in line with this theory. The molecule has altogether 5 "*lone pair"* electrons.

Ozone has a melting point of -192.7°C and a boiling point of –111.9°C. It is a strongly oxidizing gas and can be a threat to both humans and vegetation.

2.3. Formation of ozone

Molecular oxygen is very stable and is present in large amounts (21% by volume) in the atmosphere. Ozone can be formed when **atomic** oxygen reacts with ordinary **molecular** oxygen. The reaction takes place in a two-step process according to the following reaction scheme:

$$O_2 + h\nu \Rightarrow O + O \qquad (2.1)$$

$$O + O_2 + M \Rightarrow O_3 + M \qquad (2.2)$$

In reaction (2.2) M is a reaction partner (e.g. nitrogen molecule). This is an important catalyst, but is not changed or used in the reaction.

The photons $h\nu$ in reaction (2.1) must have an energy of at least **5.115 eV** in order to split the oxygen molecule. This energy corresponds to photons with wavelength of 242.4 nm or shorter

Only UV with wavelength shorter than 242.4 nm can split the oxygen molecule!

UV-radiation with sufficient energy to split oxygen is absorbed high up in the atmosphere. Thus, the ozone formation is most efficient at heights around 40 km.

Atomic oxygen plays a key role in the production of ozone. When atomic oxygen is produced in the atmosphere by e.g. lightening or photochemical reactions, ozone may be formed from reaction (2.2).

2.4. Tropospheric and stratospheric ozone

Ozone may be formed in the troposphere when oxygen is released from nitrogen dioxide (NO_2) by photolysis. In this process it is not required the same amount of energy as for the splitting of the oxygen molecule. In large cities with a lot of traffic photochemical smog (containing e.g. NO, NO_2 and ozone) is formed.

A smog episode often starts with the release of NO-gas from cars. The gas is then oxidized to NO_2, which has the red-brown colour of smog. When the NO_2-molecule is exposed to sunlight an oxygen atom may be released and ozone is formed. The process can be described by the following reaction scheme:

$$2NO + O_2 \Rightarrow 2NO_2 \quad (2.3)$$

$$NO_2 + h\nu \Rightarrow NO + O \quad (2.4)$$

$$O + O_2 + M \Rightarrow O_3 + M \quad (2.5)$$

As mentioned in Chapter 1.3 we usually distinguish between stratospheric ozone and the ozone near the ground (tropospheric ozone). Tropospheric ozone has increased in recent years and can represent a problem for health and environment. Because ozone is a poisonous and oxidizing gas it attacks double bonds in chlorophyll and rubber. Ozone can even be used instead of chlorine to treat drinking water. A plant that easily is damaged by ozone is the tobacco plant "BelW3". This plant was earlier used as a monitor for the amount of tropospheric ozone. The ozone damage was represented by the number of brown spots on the leaves.

Contrary to troposheric ozone, stratospheric ozone is important for life on Earth since it absorbs parts of the UV-radiation from the sun.

The total amount of ozone in the atmosphere is called "*the thickness of the ozone layer*". It is also denoted "*total ozone column*" of just "*total ozone*". The thickness is measured in ***Dobson units (DU).***

Dobson unit

The unit adopted for quantifying the total ozone column is called **Dobson unit (DU)**. It is defined in the following way:

If the total amount of ozone over a certain area is compressed at standard temperature and pressure, it will form a layer which is 2 to 5 mm thick.

A layer of 1 mm is defined as 100 DU. The ozone layer is normally between 200 and 500 DU.

2.5. Distribution of ozone in the atmosphere

Atmospheric ozone is formed when UV-radiation with sufficient energy hits the oxygen molecules in the atmosphere. The main formation takes place in regions where the solar radiation is most efficient, i.e. in high altitude regions around the equator.

Since ozone is a gas it will be distributed around the world by the wind system. This implies that the thickness of the ozone layer changes from one place to another. Furthermore, the ozone distribution varies with altitude.

We usually distinguish between *vertical* and *global* distributions.

2.5.1. The vertical distribution

Figure 2.2 shows the vertical distribution of ozone under normal conditions. The curves represent the mean values of weekly measurements in Sodankylä, Finland (located close to the Polar circle). The measurements are carried out with balloons and ozone sondes.

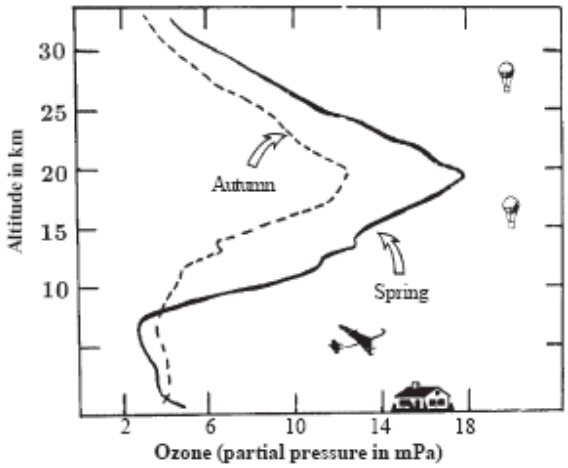

Figure 2.2: *Vertical distribution (given as partial pressure) of ozone at two different periods of the year, measured at the Finnish meteorological station Sodankylä in northern Finland. The data are average values of ozone sonde measurements.*

It can be seen from Figure 2.2 and Figure 1.1b that the atmospheric ozone is vertically distributed from the ground and up to about 55 km. The maximum concentrations are normally found between 15 km and 25 km. Furthermore the total concentration of ozone is significantly higher in spring than in autumn. Figure 1.1b also demonstrates that the vertical ozone distribution in the tropics normally is different from the distribution at higher latitudes.

2.5.2. The global distribution

It is difficult to visualize the global distribution and seasonal ozone variations from a two-dimensional figure since the ozone column varies both with latitude, longitude and time of the year. In Figure 2.3 the average global ozone distribution at different latitudes and seasons is presented. Since the Earth's topography is of large importance for the wind systems there are also large longitudinal variations, which are not shown in Figure 2.3. For example, if we follow the 60° latitude around the world it can be shown that Scandinavia has lower ozone values than Siberia and Alaska. This is particularly true during the winter-spring period.

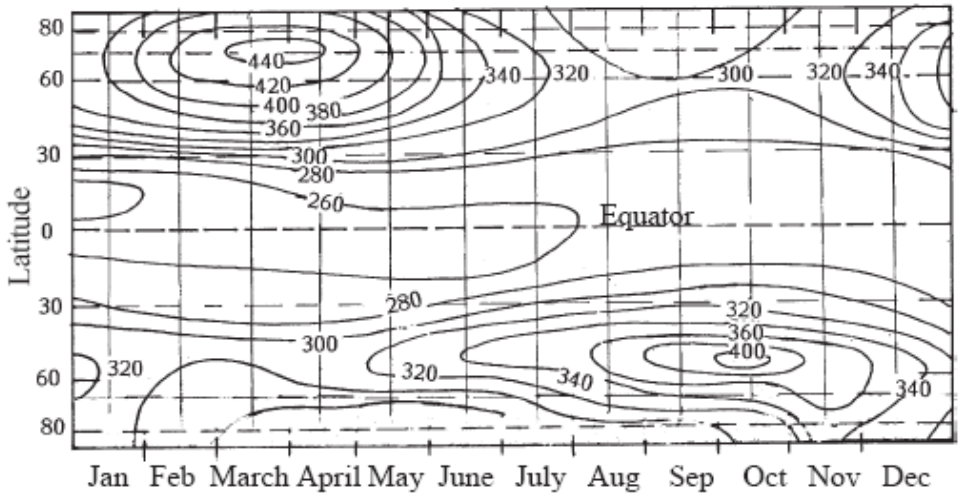

Figure 2.3: *The global latitudinal distribution of ozone and its seasonal variation. The numbers in the contour plot are average ozone values (in DU).*

Figure 2.3 demonstrates three important features about the ozone layer:

1. There is a considerable latitudinal variation of total ozone. The highest values are found at approximately 60° to 70° N and at about 50° to 60° S.
2. The ozone layer shows a large seasonal variation. The highest values are found during the spring.
3. The ozone layer is considerably thinner in the tropical regions than at higher latitudes (see also Figure 2.5).

The low ozone values around equator are somewhat surprising since the stratospheric ozone production is largest in the tropical regions. The main reason for this distribution is the wind systems. At the poles the stratospheric winter temperature is very low because solar absorption by ozone is absent. The temperature gradient leads to a global transport of ozone away from the tropics and towards polar latitudes in the winter hemisphere. Consequently, low column ozone values are consistently observed in the tropics and maximal ozone occur at polar latitudes in the late winter or early spring. This so-called Brewer-Dobson circulation, in which air rises in the tropics and then moves polewards and downwards as visualized Figure 2.4.

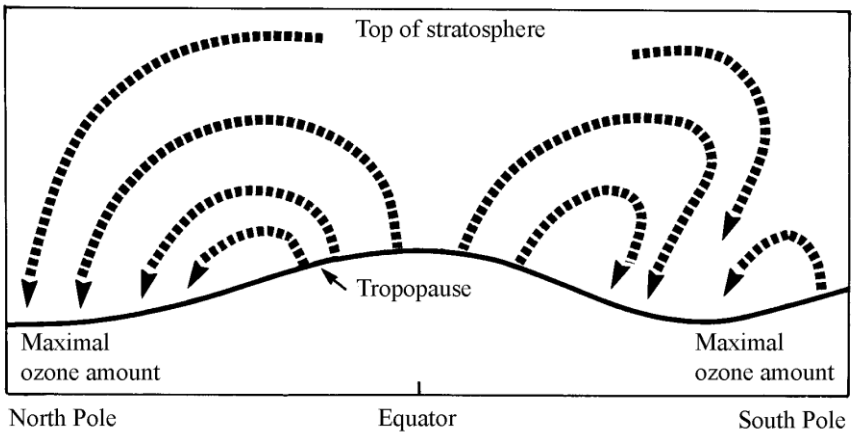

Figure 2.4: *Transport of ozone from lower to higher latitudes in the stratosphere (Based on Figure in Stordal and Hov, 1993).*

In Figure 2.5 the annual average ozone variation for Hawaii and Oslo is presented. The latitudinal positions for the two places are 19°N and 60°N, respectively. In Hawaii the annual ozone variation is approximately 10%, whereas in Oslo the variation is about 40%, with the highest values in March and April. Furthermore, the ozone layer above Hawaii is about 30% thinner than the layer above Oslo.

In order to evaluate the environmental effects of the ozone layer it should be noted that the spring and summer seasons, when the sun is high, are most important. As you can see from Figure 2.5 the average ozone layer can vary a lot during these months. At high latitudes (Norway) the ozone values reach a maximum of about 400 DU in April and decrease gradually to about 280 DU in late October. As will be shown in Chapter 4 the day to day variations of the ozone layer can be even larger.

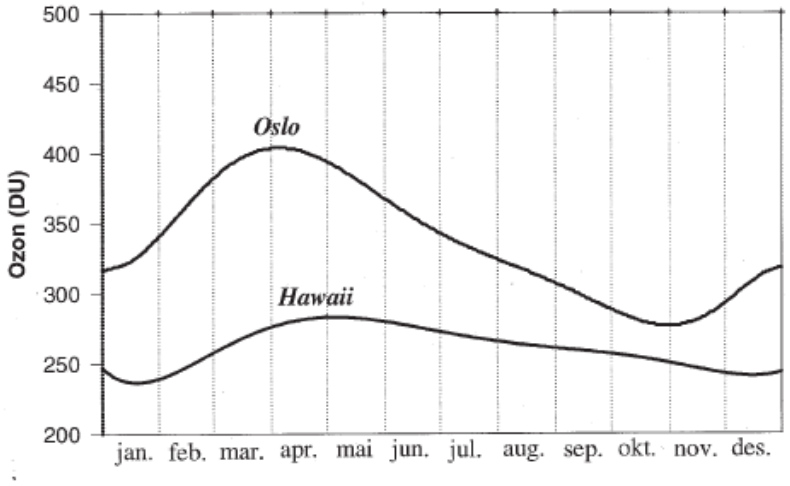

Figure 2.5: *The annual average variations of the ozone layer above Hawaii and Oslo. The two curves refer to the period 1980 to 1990.*

Chapter 3

Ozone measurement techniques

3.1. Ozone observations

This chapter describes how we can measure the amount of gas that is mixed with a number of other gases and distributed over a region stretching from the ground and up to an altitude of about 50 km.

We need "something" which can reach the ozone layer and interact with ozone. Furthermore, we must be able to observe this interaction.

When UV-radiation passes the ozone layer a certain fraction is absorbed. The absorption increases with the amount of ozone between the sun and the instrument. Consequently, we can use the absorption of UV as a measure for the ozone concentration. The wavelength region from about 300 nm to about 330 nm is best suited for the measurements. It is also possible to use the Chappius band in the visible region (see Figure 1.3) for ozone measurements. Since the absorption in the visible region is weak the observations requires a large "air mass" (the sun must be low or near the horizon) in order to attain optimal measurements. In the next chapters we will describe the physical basis for the ozone measurements.

3.1.1. The physical foundation

The intensity of radiation when it hits a substance (e.g. the atmosphere) is often called I_0. The substance absorbs and scatters radiation and the intensity I is gradually attenuated as the radiation penetrates the material. For a substance with attenuation coefficient k the intensity of radiation that has travelled a distance s is given by the equation:

$$I = I_0 e^{-ks} \tag{3.1}$$

In Figure 3.1 the transport of UV-radiation through the atmosphere is visualized. As a first assumption we assume that the sun is in zenith (straight above our head) and that the radiation travels vertically through the atmosphere and is partly absorbed by the ozone layer. Furthermore, the radiation is scattered from the molecules in the air (called *Rayleigh scattering*) and from dust and small particles (called *Mie scattering*).

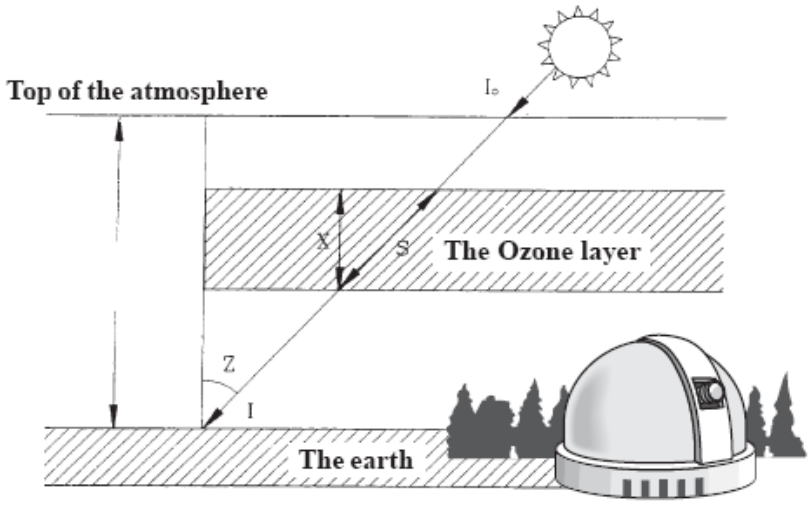

Figure 3.1: *The principle for ozone measurements. The slant path of the sun increases the effective thickness of the ozone layer from X to S=μX.*

If these three effects are taken into account we can determine the intensity of the radiation passing vertically through the atmosphere:

$$I = I_0 e^{-\alpha x - \beta - \delta} \qquad (3.2)$$

Here x is the thickness of the ozone layer (the quantity which we want to determine), α is the absorption coefficient for ozone (absorption per unit length), β is the Rayleigh scattering coefficient for the whole atmosphere and δ is Mie scattering from dust and particles in the atmosphere.

Equation 3.2 represents solar radiation from zenith. In reality the solar rays have a slant pathway through the atmosphere and the intensity at the ground depends on the solar zenith angle. According to Figure 3.1 the pathway through a plane parallel atmosphere will increase with a factor μ (called air mass) given by:

$$\mu = \frac{1}{\cos Z}$$

where Z is the solar zenith angle. The UV intensity at the ground for solar zenith angle Z and air mass μ is:

$$I = I_0 e^{-\alpha\mu x - \beta\mu - \delta\mu} \qquad (3.3)$$

Figure 1.3 shows the absorption spectrum for ozone. In order to determine the thickness of the ozone layer we usually measure UV with wavelengths in the Huggins absorption band. The thickness of the ozone layer x can in principal be determined when the different parameters in equation (3.3) (α, β, δ and I_0) are known.

Wavelengths used in ozone retrievals

It is fairly difficult to measure the absolute intensity of UV at a certain wavelength. Thus, we normally measure the relative UV intensity of two or more wavelengths that are differently absorbed by ozone. Wavelength pairs (λ and λ') commonly used by the standard Dobson instruments are:

NAME	WAVELENGTH (in nm), λ	WAVELENGTH (in nm), λ'
A	305.0	325.0
B	308.8	329.1
C	311.5	332.4
D	317.5	339.9
C'	332.4	453.6

The shortest wavelength λ vary from 305 nm to 332.4 nm. In the wintertime when the sun is low at high latitudes, the UV-radiation is very weak at wavelength 305 nm. Consequently, it is difficult to use the A-pair during winter at stations located at latitudes higher than about 50°. Instead the less accurate C-pair can be used at these stations.

Measurements of ozone

Equation (3.3) can be used for the two wavelengths λ and λ', with corresponding intensities I and I'. The logarithms of Equation (3.3) give:

$$\ln I = \ln I_0 - (\alpha x + \beta + \delta)\mu \qquad (3.4)$$

$$\ln I' = \ln I'_0 - (\alpha' x + \beta' + \delta')\mu \qquad (3.5)$$

By subtracting equation (3.4) from (3.5) we get:

$$\ln(I'/I) = \ln(I'_0/I_0) + (\alpha - \alpha')\mu x + (\beta - \beta')\mu + (\delta - \delta')\mu \qquad (3.6)$$

The scattering from dust and particles (given by the scattering coefficient δ) varies little with wavelength. This implies that (δ-δ') is close to zero and that Mie scattering can be ignored. Equation (3.6) can be solved with respect to x and we get the following expression for the thickness of the ozone layer:

$$X = \frac{\ln(I'/I) - \ln(I'_0/I_0)}{(\alpha - \alpha')\mu} - \frac{\beta - \beta'}{\alpha - \alpha'} \qquad (3.7)$$

In order to determine the ozone thickness, the intensity ratio I´/I is measured from the instrument. Furthermore, the latitude, longitude, time and date are used to calculate the solar zenith angle and airmass μ. The physical constants α, α', β and β' depend on the slit width of the instrument and the wavelength of radiation. Only one problem remains, namely the parameter $ln(I'_o/I_o)$ which represents the intensity ratio outside the Earth's atmosphere.

Determination of the parameter $ln(I'_o/I_o)$

The intensity ratio $ln(I'/I)$ is a linear function of air mass μ if the ozone layer x is considered constant. From equation (3.7) we get the following expression:

$$\ln(I'/I) = [(\alpha - \alpha') + (\beta - \beta')x]\mu + \ln(I'_0/I_0) \qquad (3.8)$$

During a day the parameter μ will change in accordance with the solar elevation. If x is constant during the day (this is often true for stable weather situations) the intensity ratio $ln(I'/I)$ will form a straight line in a plot with $ln(I'/I)$ and μ along the axes (see Figure 3.2):

$$\ln(I'/I) = k \cdot \mu + \ln(I'_0/I_0) \qquad (3.9)$$

The straight line in Figure 3.2 can be extrapolated to $\mu = 0$. In practice this is an unrealistic experimental value since the smallest obtainable value for the airmass is $\mu=1$ (when the sun is in zenith). Still, an experimentally observed line which passes through $\mu=0$ gives the value we need

$$\mu = 0 \Rightarrow \ln(I'_o/I_o)$$

In most ground based instruments a combination of two wavelength pairs are used. The purpose is to further reduce the influence of scattering from particles in the atmosphere. In standard Dobson ozone measurements the A and D pairs are combined. This is called AD measurements.

For μ-values larger than about 4 (zenith angles larger than 75°) the sun is too low and the UV-radiation too weak to perform reliable ozone measurements. At these conditions other measuring methods can be used.

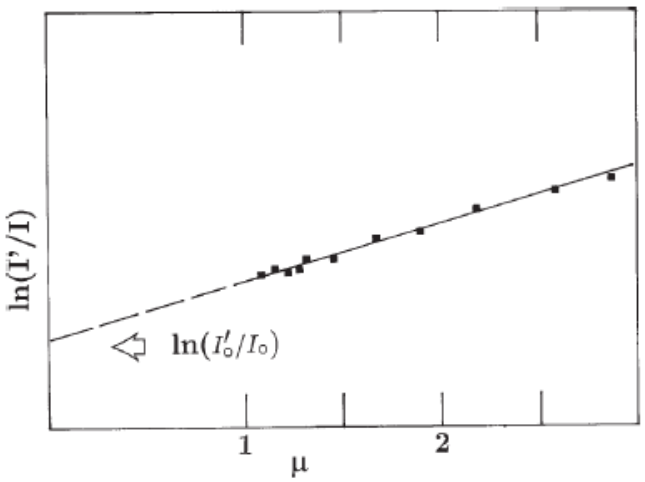

Figure 3.2: *For constant ozone and airmass smaller than 3.5 (zenith angle smaller than 73°) the intensity ratio ln (I'/I) varies linearly with μ.*

The world is not flat

In the procedure described above we have assumed that the Earth is flat. It will be a small correction to equation (3.7) when we take into consideration that the Earth is spherical. This correction is especially important at large solar zenith angles.

3.2. Ground based instruments

Most ground based instruments use visible or UV-radiation from the sun to measure the total ozone column in the atmosphere. However, it is also possible to use light from the moon (on days around full moon) or from stars. These methods are valuable supplements to the traditionally ozone measurements in the wintertime at high latitudes with polar nights. On overcast days it is also possible to perform good ozone measurements from scattered light from zenith (zenith measurements).

The different types of ground based measurements have different uncertainties. Normally we have highest confidence in measurements based on direct solar radiation in the UV region. However, such measurements can only be performed on clear days when the solar disk is visible. The zenith light method has improved significantly during the last years, thanks to applications of radiative transfer models. The theory of atmospheric radiative transfer will be described briefly in Chapter 7.

On the next pages you will have an overview of the most important types of ground based ozone instruments used today.

3.2.1. The Dobson instrument

In the late 1920s the photocell was invented and the radio tubes became available. G.M.B. Dobson realized that this technical progress would revolutionize the measuring technique. A method of measuring the ozone layer directly, without using photography, would now be possible. In 1928 the first photoelectrical instrument for ozone measurements was ready for testing. This instrument was the well-known Dobson spectrophotometer or simply the Dobson instrument (see Figure 3.3). This instrument was produced by Beck's in London.

Altogether about 150 Dobson instruments have been made and all of them are equipped with a certain production number. The Oslo instrument that was used until 1998, had serial number 56. Two other Norwegian Dobson instruments, used in Tromsø and Svalbard, have serial numbers 14 and 8.

Today approximately 100 Dobson instruments are in operation throughout the world, mainly on the Northern Hemisphere and north of 30°N.

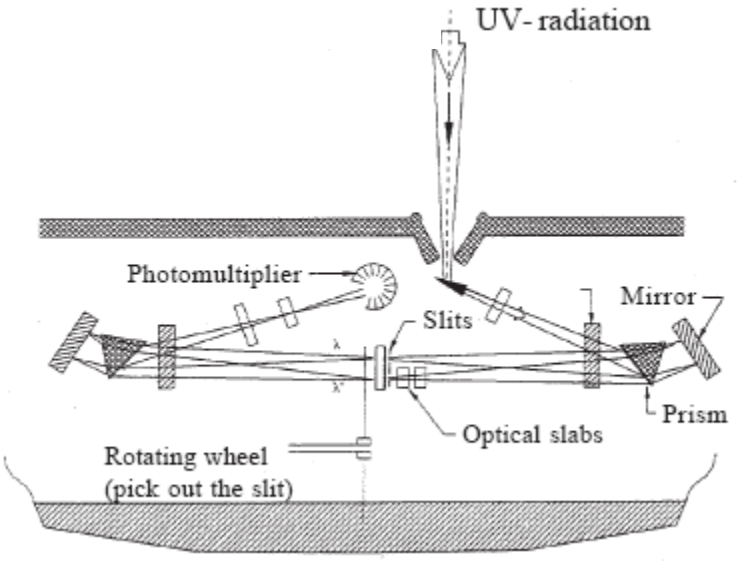

Figure 3.3: *A drawing of the Dobson instrument which is about 1.5m long. The illustration shows the light passage through the instrument. Two wavelengths λ and λ' are separated by a prism. An optical slab is gradually inserted to reduce the intensity of λ'. When the photomultiplier shows zero current (I=I') a dial reading, connected to the optical slab, can be registered. This number is proportional to ln(I'/I).*

The Dobson instruments are quite stable and have been used routinely for about 80 years. Thus, in order to make ozone trend analysis for periods of more than 30 years we have to trust data from the Dobson instruments.

From time to time the instruments are brought together for calibration purposes. The world standard Dobson instrument has fabrication number 83 and is placed at the Mauna Loa observatory on Hawaii.

The Dobson instruments are operated manually (or partly manually) and it takes normally 20 to 30 minutes to perform a series of measurement.

3.2.2. The Brewer instrument

From 1982 another ground based instrument became available: the so-called Brewer instrument. The picture below shows the Brewer instrument operating in Oslo. The main difference between the Dobson and Brewer instruments is that Brewer is fully automatic and can perform measurements according to a programmed schedule.

The Brewer instrument placed at the roof of the Physics building at the University of Oslo. To the left you can see the entrance window for solar radiation. The window is always directed towards the sun. On the top of the instrument (left side) you can see the quartz dome used for global irradiance measurements.

The Brewer instrument is equipped with a tracking system and can "follow the sun" during the day. The PC and data logger connected to the instrument is placed indoors.

The Brewer instrument can also measure other atmospheric gases, such as NO_2 and SO_2. Furthermore, a particular unit makes it possible to measure spectral UV-radiation from 290 nm and up to 372 nm. The UV spectra contain direct and scattered radiation entering the quartz dome at the top of the instrument. In recent years algorithms for retrieving aerosol optical depth (AOD) have also become available. It should be mentioned that Arne Dahlback (University of Oslo) has developed routines for retrieving ozone values from global irradiance data, i.e. direct and diffuse radiation entering the quartz dome.

3.2.3. GUV and NILU-UV instruments

Another common instrument used for ozone measurements is GUV (Ground-based ultraviolet) filter radiometer. This is a 5 channel instrument designed to measure UV irradiances in 4 channels, with centre wavelengths at 305 nm, 320 nm, 340 nm and 380 nm. The bandwidths are approximately 10 nm FWHM (Full Width at Half Maximum). The fifth channel is a PAR channel (Photosynthetically Active Radiation, 400-700 nm). The instrument is manufactured by Biospherical Instruments Inc, USA. The GUV instrument is temperature stabilized at 40°C and has a time resolution of 1 minute. Using a technique developed by Dahlback (1996), it is possible to derive total ozone abundance, cloud cover information, UV spectra from 290 nm to 400 nm and biologically weighted UV-doses for several action spectra in the UV. At the University of Oslo a GUV-511 instrument has been in continuous operation since 1994.

Another instrument, NILU-UV, is based on the same principals as the GUV. The total (diffuse and direct) incoming UV irradiance is measured in five channels with centre wavelengths at 305 nm, 312 nm, 320 nm, 340 nm, and 380 nm. Each channel bandwidth is about 10 nm. A sixth channel covers the PAR.

3.2.4. The SAOZ instrument

Around 1990 it was constructed a French ozone instrument, SAOZ, which is quite different from other ground based instruments. First, the light is measured by a number of diodes and not by a photomultiplier. Secondly, the instrument uses visible light around 510 nm in the Chappius band (see Figure 1.3). The measurements are based on zenith light and the name of the instrument, SAOZ, originates from the French name "*Systéme d'Analyse et d'Observations Zénithales"*. Since the absorption in the visible part of the solar spectrum is very weak, the path through the atmosphere and ozone layer must be long in order to get as large absorption as possible. The instrument requires low sun and can therefore be used to measure total ozone at high latitudes during winter.

3.3. Satellite measurements

Regular ozone measurements from satellite started in October 1978 when the satellite Nimbus 7 was launched. Now it was possible to measure the ozone layer from "the outside". In this chapter we will briefly describe some satellites and their measuring techniques.

1. Backscattered UV-radiation from the sun

The satellite can look vertically down to the Earth (nadir) and observe the radiation backscattered from the atmosphere (Rayleigh-scattering). In principle this is similar to the zenith light measurements used for ground based instruments. The technique is called SBUV, an abbreviation for "*Solar Backscatter UV"*. The ozone instrument onboard the satellite Nimbus 7 used 12 different wavelengths in the region from 250 nm to 340 nm. By combining all these wavelengths it was possible to retrieve information about both the vertical distribution as well as the total amount of ozone. An essential part of the retrieval of total ozone and ozone profiles is the use of an adequate radiative transfer model (RTM).

2. Infrared radiation from the Earth

In Chapter 1.5 it was mentioned that the Earth is like a black body with a temperature of about 288 K. The emitted radiation is in the infrared region with a maximum around 10 μm. Ozone has an absorption band around 9.6 μm, thus the satellites can measure the Earth's emitted radiation to determine the amount of ozone. The measurements are similar to the direct solar measurement method described for ground based instruments. However, this method is more uncertain than the "backscatter method" because other gases in the atmosphere (e.g. water vapour) absorb in the infrared region. An advantage with this method is that it is independent of daylight and can be used to observe ozone in the polar region during the wintertime (the polar night).

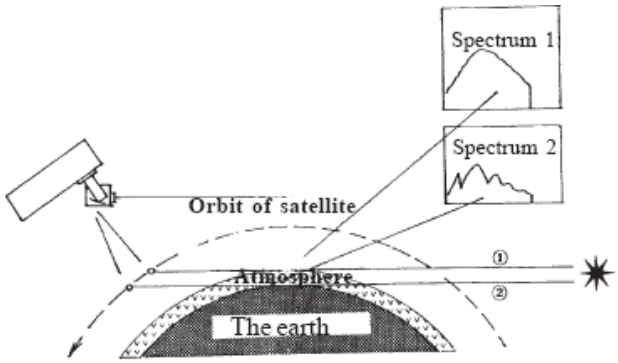

Figure 3.5: *The GOMOS system. Ozone is measured with the help of occulting stars. The observations are based on the differences in the light spectra when the star is observed from the outside of the atmosphere (1) and when the light has passed the whole atmosphere (2).*

3. Light from the stars

GOMOS (*Global Ozone Monitoring by Occultation of Stars)* is a high resolution spectrometer covering the wavelength range from 250 nm to 950 nm. The instrument is based on light from the stars (see Figure 3.5).

The light from the stars, when it disappears under the horizon, can provide information about total ozone. The light spectrum is compared to the spectrum obtained when the starlight is measured outside the atmosphere (the two spectra 1 and 2 in Figure 3.5). In addition to ozone the GOMOS system can be used to observe e.g. NO_2, ClO and SO_2. There are approximately 40 stars that can be used for this type of measurements.

3.3.1. Global ozone measurements

The satellite orbits are normally from 500 km to about 800 km above the Earth. The instruments are looking down at the Earth and consequently a large area can be observed within a day. This is in contrast to the ground based instruments, which only measure at one single location. A drawback with the satellites is the problems with calibration and repair after they have been launched. Slowly developing changes in the instruments are often difficult to detect. This happened to the Nimbus 7 satellite, where the properties of a "*diffuser plate"* in the TOMS instrument changed slowly.

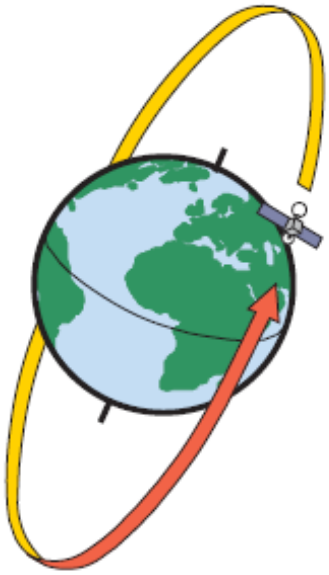

It is a complicated task to measure total ozone from satellite. In the first years the observations were hampered with large uncertainties. However, the methods used for calibration and control have gradually improved and the confidence to the results have increased significantly during the last years.

TOMS

The most famous satellite ozone instrument is called TOMS, an abbreviation for "*Total Ozone Mapping Spectrometer"*. The amount of ozone is determined by comparing the direct radiation from the sun with the backscattered radiation from the atmosphere. The radiation from the sun is scattered by molecules in the air as well as clouds. The instrument registers solar radiation at several different wavelengths. The TOMS measurements cover a surface area of 50 to 200 km along a line perpendicular to the motion of the satellite. Approximately 200 000 daily measurements cover most of the Earth, except for areas near the pole where the sun is low or below the horizon.

The TOMS measurements have been performed by NASA (*National Aeronautics and Space Administration*) and altogether 4 different instruments have measured ozone for longer or shorter periods since 1978:

1. The first TOMS instrument was launched with the **Nimbus 7** satellite in October 1978. It was in operation until May 1993, almost 15 years.

2. The second TOMS instrument was launched with the Russian satellite **Meteor 3**. It was in operation from August 1991 until 27th of December 1994.

3. It was a period of about 1.5 years with no ozone measurements before the third TOMS instrument was launched onboard the satellite **Earth Probe**. The launch was planned for 1994, but we had to wait until 2nd of July 1996 before the satellite came into a circular orbit at an altitude of 500 km. From this altitude it was also possible to study UV absorbing aerosols in the atmosphere. Because of the low orbit altitude it is impossible to cover the total atmosphere during a day, particular in tropical regions. The TOMS instrument onboard Earth Probe is still in operation, but it is currently experiencing calibration problems.

4. The 17th of August 1996 the Japanese satellite **Adeos** was launched with the 4th TOMS instrument onboard. The orbit had an altitude of 800 km and a revolution time of 100 minutes. The measurements went on until the end of June 1997.

Other ozone measurements from satellite

In addition to the TOMS instrument on Earth Probe the Ozone Monitoring Instrument (**OMI**) onboard AURA, are currently the only NASA spacecraft on orbit specializing in ozone retrieval. OMI ozone data "over your head" are available from September 2004 until present (see http://jwocky.gsfc.nasa.gov/teacher/ozone_overhead_v8.html).

In addition to the NASA spacecrafts, the European Space Agency (ESA) has other ozone monitoring instruments onboard their satellites:

* **GOME** (Global Ozone Monitoring Experiment) is a nadir-scanning ultraviolet and visible spectrometer for global monitoring of atmospheric ozone. It was launched onboard ERS-2 in April 1995 and operated until 2003. A second GOME instrument onboard MetOp was launched in 2007.

* **SCIAMACHY** onboard the ESA satellite ENVISAT is a spectrometer (240 nm - 2380 nm) whose primary mission objective is to perform global measurements of ozone and other trace gases in the troposphere and stratosphere. It has been in operation since 2002.

The ozone measurements from satellite are presented as daily global maps. Different colours are used to visualize the amount of ozone. This makes it possible to study regions with low or high concentrations of ozone and to follow the movement of these special areas. The ozone measurements are published on internet and are public available short time after the overpass.

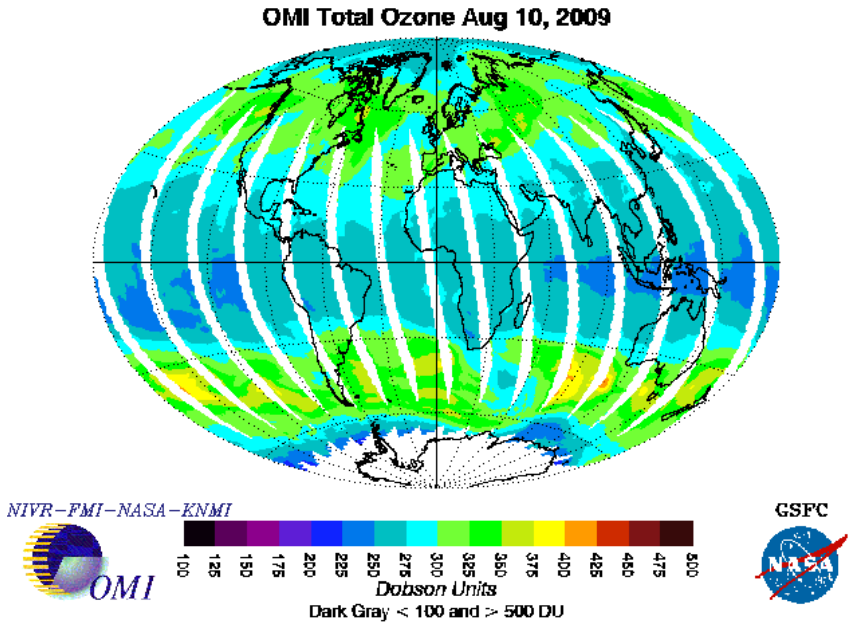

Figure 3.6: *Global ozone maps from OMI August 10, 2009. The maps are available at* http://macuv.gsfc.nasa.gov/.

3.4. Observations of the vertical profile

When Dobson started his pioneer studies of atmospheric ozone it was assumed that the gas had the maximum concentration at an altitude of about 40 km. This assumption was not based on measurements, rather a "guess" since no methods were available for observation of the vertical profile. This uncertainty worried Dobson because an error in the vertical profile would give errors in the ozone retrievals (the path through the ozone layer would be wrong). Today we have different methods to determine the ozone profile, including balloons with ozone sondes, satellites and lidars.

The altitude of the ozone layer was first determined from ground based observations. It all started with F.W.P. Götz, a good friend of Dobson, in the summer of 1929 at Spitzbergen (Svalbard). He discovered that the ratio of zenith sky radiances of two wavelengths in the ultraviolet, one strongly and the other weakly absorbed by ozone, increased with increasing solar zenith angles but suddenly decreased at zenith angles close to 90º. Götz named this observation the "Umkehr effect" and realised that such measurements contained information about the vertical distribution of ozone in the stratosphere.

The first serious observations, using the Umkehr-method, were carried out in Switzerland in 1932. The results showed that the gas was not located at 40 to 50 km. Instead, most of the gas was found in the region from 15 to 35 km, with the maximum concentration at approximately 22 km.

In the 1960s rockets were used to observe the vertical profile of ozone. The experiments revealed large day/night variations in the ozone layer at altitudes of 50 to 60 km.

3.4.1. Ozone measured with balloons

In order to get information about the vertical profile of ozone it is possible to use balloons. A balloon filled with Helium or Hydrogen can bring an ozone instrument to the altitudes where the ozone layer is located (see Figure 3.7). The balloon observations are mainly based on a chemical determination of ozone and the observations are made continuously as the balloon ascends. This will give the vertical profile as well as the total amount of ozone by integrating all individual observations.

The balloons will normally reach altitudes of approximately 30 km. Thus, the sondes do not measure the upper part of the ozone layer. Instead qualitative assumptions of the upper ozone profile are made.

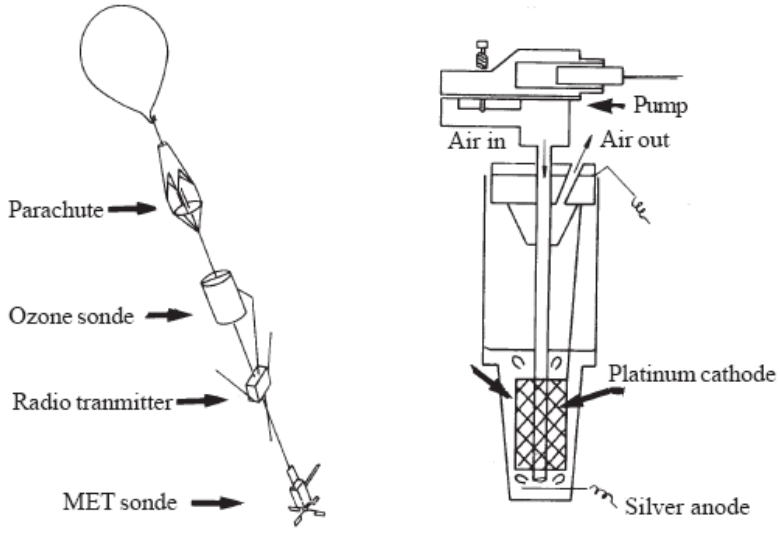

Figure 3.7: *An ozone sonde carried by a balloon. To the right is the ozone instrument and to the left is the balloon with all its equipment. A MET sonde contains the meteorological equipment. The data are transmitted to a receiver via radio.*

3.4.2. Lidars

LIDAR (Light Detection and Ranging) is an optical remote sensing technology that measures properties of scattered light to find information of a distant target. The prevalent method to determine distance to the object (e.g. ozone) is to use laser pulses.

Today ozone lidars are frequently used to measure ozone profiles. One such lidar is located at the ALOMAR Observatory at Andøya. This instrument is run on a routine basis under clear sky conditions, providing ozone profiles in the height range 10 to 45 km.

The measurements are based on the DIAL (differential absorption lidar) technique which enables the average concentration of the absorbing gas, in this case ozone, to be detected at different altitudes by measuring the difference in the lidar backscattered signals for two laser wavelengths. The pulses of 308 nm and 353 nm radiation propagate through the atmosphere simultaneously. As they propagate, radiation at both wavelengths are scattered and absorbed. Radiation at 308 nm is more strongly absorbed by ozone; the strength of its backscattered signal therefore decreases with height more rapidly than that of radiation at 353 nm. The difference in the return signal strengths at the two wavelengths can be related to the ozone concentration.

Chapter 4

Ozone measurements and trends

4.1. Introduction

In the last chapter we discussed the different methods used to observe ozone. Today the ozone layer is measured several times each day from a large number of stations around the world. Furthermore, satellite observations are used to map the global ozone distribution.

The ozone layer is not constant, but can vary considerably from one day to another, from season to season, and with geographical position. The last decades there has been much focus on the ozone holes and an ozone depletion that is observed at most latitudes. The depletion may be due to a) changes in the formation of ozone, b) changes in the destruction of ozone, or c) changes in the global ozone distributions due to meteorological changes.

One of the main issues in the ozone debate is the longtime trend of total ozone. At most stations it is observed a gradually decrease in the ozone layer from the latter part of the 1970s until the end of the 1990s. In this chapter we give you some examples of measurements and longtime trend of the ozone layer.

4.2. Ozone measurements in Oslo

4.2.1. Daily observations

Figure 4.1 shows the daily ozone observations from the ground based Brewer instrument in Oslo for the year 2008. As seen from the figure the ozone layer can vary considerably from one day to another. In February and March 2008 the ozone values increased from 230 DU to almost 500 DU in just a few days. The lowest ozone values are normally observed in the late fall, whereas the ozone maxima usually occur in the spring. The large seasonal variations are typical for stations at high latitudes. This is a dynamic phenomenon and is explained by the springtime transport of ozone from the source regions in the stratosphere above the equator.

The blue line in Figure 4.1 represents the average ozone value from 1978 to 2006. As we can see from the figure the ozone values in 2008 were fairly close to the average values most of the year.

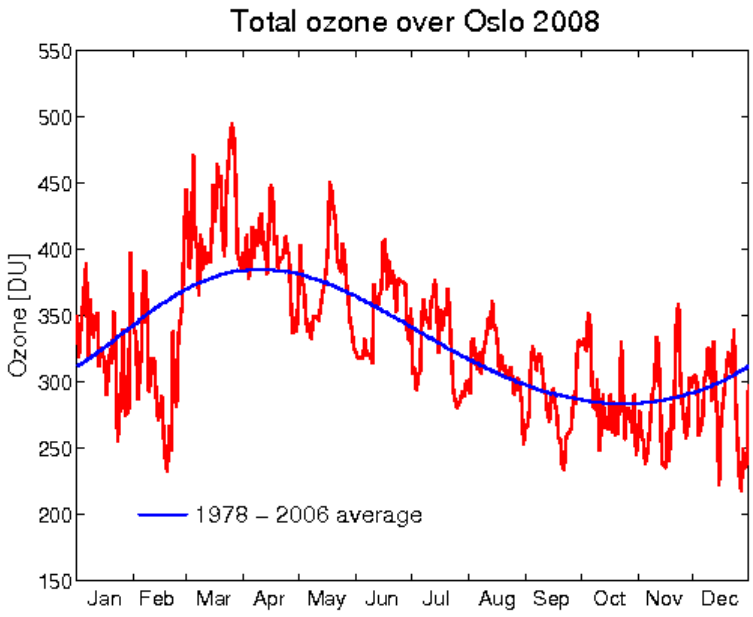

Figure 4.1: *Daily measurements of total ozone in Oslo in 2008. The blue line is the average value for the period 1978 to 2006.*

4.2.2. Ozone trends for Oslo

Total ozone measurements using the Dobson spectrophotometer (No. 56) was performed on a regular basis in Oslo from 1978 to 1998. In the summer 1990 the Brewer instrument was installed at the University of Oslo to gradually replace the Dobson instrument.

Figure 4.2 shows the variations in the monthly mean ozone values in Oslo from 1979 to 2007. The total ozone data from 1979 to 1997 are from the Dobson instrument, whereas the Brewer data have been used for the 1998-2007 period.

In order to look at possible ozone trends for the period 1979 to 2007 the seasonal variation is removed by subtracting the long-term monthly means and adding the long-term yearly mean ozone value. A simple linear regression has been fitted to the data to obtain a long-term ozone trend. For the spring a significant negative trend of –0.21%/year is observed. For the winter, summer and fall no significant trend is observed. When all months are included in the analysis a significant negative ozone trend of –0.12%/year is observed above Oslo. As a comparison it is interesting to note that the annual ozone trend for the period 1978-1998 was -0.42%/year, with a winter/spring ozone decrease as high as –0.62%/year! Thus, the last winters with "high" ozone values have reduced the annual downward trend significantly.

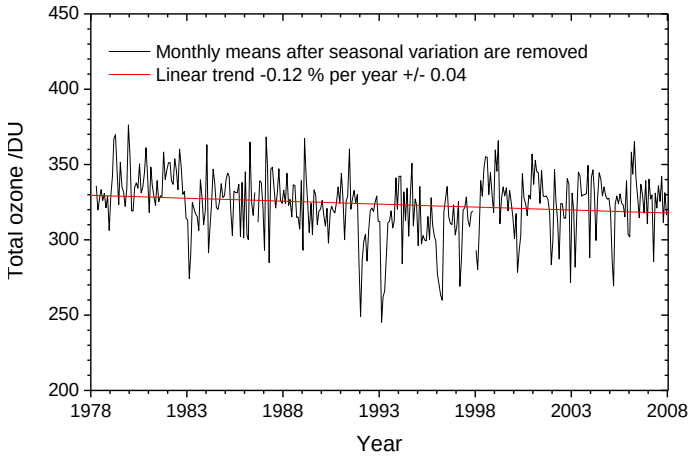

Figure 4.2: *Variation in total ozone over Oslo for the period 1979–2007. The seasonal variations have been removed from the plot. A linear downward ozone trend of –0.12%/year is observed (Source: NILU/SFT report, 2007).*

4.3. Time series from Arosa, Switzerland

A large number of ozone observations from hundreds of stations have been performed during the last 30 year. However, only a few continuous time series are available from the period 40 to 80 years back in time.

The total ozone series of Arosa, Switzerland (46.8°N, 9.68°E, 1820 altitude) is the longest in the world. The measurements started in 1926 by F. W. P. Götz. Thus, this ozone record is very important to attain information about the ozone layer and its variations before the release of CFC-gases started.

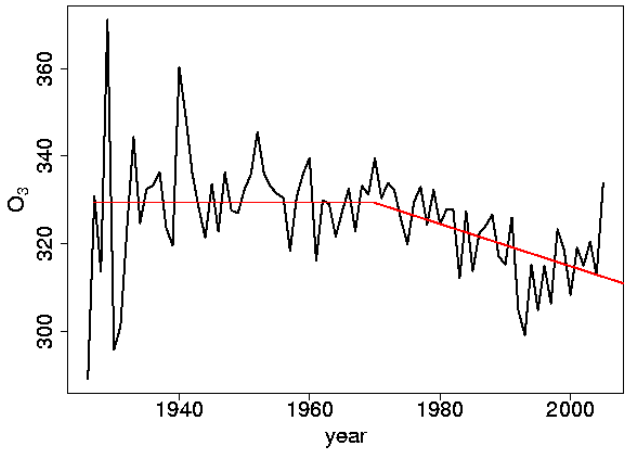

Figure 4.3: *Ozone observations from Arosa, Switzerland, from 1926 to 2006. The black curve represents the annual ozone mean. The ozone trend for the periods 1926-1973 and 1974-2006 are marked as red lines.*

The red straight line in Figure 4.3 indicates a possible interpretation of trend for two time periods: 1926-1973 and 1974-2006. According to the trend lines the ozone layer varied around a mean value of 330 DU all years up to 1973. From the middle of the 1970s to 2006 a significant ozone depletion of about 6% is observed. However, for the last few years the depletion process seems to have stopped. The possible ozone recovery might be related to the decreased release of CFC's and other ozone destructing substances controlled by the Montreal Protocol. This will be described further in chapter 5. Meteorological factors are other possible explanations of the ozone increase observed the last winters.

Most of the old ozone observations were originally intended as a supplement for weather forecasting and not for long-term evaluations. Consequently, a majority of the world wide measurements performed prior to 1960 are sporadic and useless for trend evaluations. However, after careful adjustments and quality checks two Norwegian ozone records have proven satisfactory for research purposes. The ozone series from Dombås (performed with Dobson #8) is one out of few records with continuous and high quality measurements from the 1940s. Also the ozone measurements from Trømsø, which started in 1935 with Dobson #14, have been of great interest in international ozone research.

4.4. Global ozone trends

In the previous chapters ozone measurements from Oslo and Arosa were presented. But how is the situation for the rest of the globe?

In the document "Scientific Assessments of Ozone Depletion: 2006" status of the ozone layer for latitudes 60°S to 60°N is described. It is concluded that the global mean total ozone values for 2002-2005 were 3.5% below 1964-1980 average values. However, the 2002-2005 values were similar to the average from 1998-2001. This behaviour is evident in all available global datasets. The report also comments that the total ozone column over the tropics (25°S-25°N) essentially has remained unchanged, whereas significant ozone depletion is observed at higher latitudes.

For the midlatitudes (35°-60°) there are differences between the two hemispheres in the evolution of total ozone:

a) For the period 2002-2005, the average total ozone for the Northern Hemisphere (NH) and Southern Hemisphere (SH) midlatitudes are about 3% and 5.5%, respectively, below their 1964-1980 average values. The NH shows an ozone minimum around 1993 followed by a small increase. The SH shows an ongoing decrease through the late 1990s followed by a recent levelling off.

b) There are seasonal differences between NH and SH in ozone changes over midlatitudes. Changes since the pre- 1980 period over northern midlatitudes (35°N-60°N) are larger in spring, whereas those over southern midlatitudes (35°S-60°S) are nearly the same throughout the year

For the Arctic and Antarctic regions the situation is different from the areas below 60°. The Arctic spring total ozone values seem to have increased slightly since the 1990s, but for the winter period the ozone decrease has continued. In winter 2005 the ozone loss was the largest ever observed. Also in Antarctica the conditions for ozone destruction are very different from those at higher latitudes. However, there are large yearly variations due to meteorological conditions. The Antarctic ozone loss or the so-called "Antarctic ozone hole" will be described in the next chapter.

4.5. The ozone hole in Antarctica

There are few other things that have had such a dramatic effect on the public and environmental organizations as the discovery of the "*ozone hole in Antarctica"*. It was J.C. Farman and co-workers, with an article in the English journal Nature in 1985, that told the world that something was going on in the stratosphere over Antarctica.

J.C. Farman, B.G. Gardiner and J.D. Shanklin;
Large losses of ozone in Antartica reveal seasonal ClO_x/NO_x interaction
Nature 315, 207 - 210 (1985)

Ozone observations made at the English station Halley Bay, located at latitude 76°S, showed that the average ozone value for October had been reduced significantly from the mid 1970s to the mid 1980s (see Figure 4.4). The spring months from September to November are periods where we normally expect the ozone values to increase. Instead, it was observed that the ozone values decreased to a minimum.

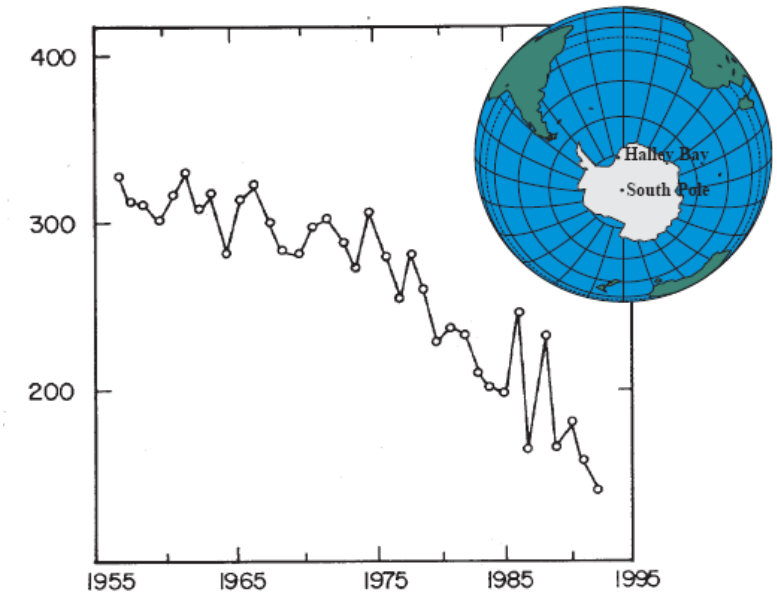

Figure 4.4: *The October average ozone values (in DU) for Halley Bay (Source: WMO/UNEP, Report-37, 1994).*

"The ozone hole" developed gradually from the beginning of the 1970s. In 1987 the average ozone value was almost 40% lower than "normal". Balloon experiments showed that the depletion was largest at an altitude of 14 to 22 km (see Figure 4.6). In this region almost all ozone was destroyed.

The discovery of the ozone hole has attained considerable attention and concern. In Antarctic it is not a question about a negative ozone trend of a few percent per decade. The depletion is very large and it returns every spring.

Today we know that the ozone hole is connected to the release of CFC-gases and the increase of chlorine in the atmosphere. Before we embark on the current explanation, we will go back in time when they started the observations in Antarctica.

"The Antarctic ozone hole" is a depletion of the ozone layer lasting from September to November.

4.5.1. The first measurements in Antarctica

The very first ozone observations in Antarctica were made by the Englishman Stan Evans in 1956, as a preparation for the *Geophysical year 1957/58*. He brought a Dobson instrument to the British research station Halley Bay. The ozone pioneer, professor Dobson, was very much involved in the experiments and he waited impatient to obtain the telegram with the first results from the Antarctic measurements.

What to expect in Antarctica?

The only experiments that would give a hint about the annual ozone variations in the Polar region were the measurements performed by Søren H.H. Larsen (who worked at the University of Oslo until 1996) at Spitzbergen, Svalbard. This island is located almost at the same latitude as the Antarctic station. The Arctic experiments, performed 6 years earlier, showed a significant increase in the ozone values in the winter and early spring. Dobson thought that the Spitzbergen data, shifted 6 months in time, would represent the annual ozone cycle in Antarctica.

The first data were a surprise!

The very first ozone observations made at Halley Bay in September and October of 1956 were approximately 150 DU lower than the corresponding observations in the Arctic. These results disappointed Dobson and he feared that the instrument was damaged during the transport to Halley Bay. But then, suddenly, in late Antarctic spring the values increased and became similar to those measured in Arctic.

Because the ozone values in the late 1956s were lower than expected, it was with great interest they followed the observations the next year. However, also this time the ozone values were very low in September to November.

It was concluded that the annual ozone cycles in Arctic and Antarctica are different. Dobson explained this from the Polar vortex[1]. At the South Pole the vortex is very stable and lasts far out in the spring months (October and November) before it collapses. Dobson assumed, quite correctly, that the vortex would prevent ozone-rich air to be transported to the Antarctic regions. Such a transport would not occur until the vortex collapsed.

Due to natural meteorological conditions the Antarctic ozone values are lower than the Arctic values during spring. However, the natural Antarctic ozone decrease observed in the 1950s is very small compared to the dramatic ozone reduction measured the last 2-3 decades!

4.5.2. Observations at the South Pole

Today extensive research is going on in Antarctica, both with regard to ozone observation and climate related activities. Norway has its own research station called "Troll". The Norwegian Polar Institute is responsible for running the station, whereas the Norwegian Institute for Air Research (NILU) has a central role in the measurements of ozone, greenhouse gases and UV radiation.

After the discovery of the extensive Antarctic ozone hole in the 1980s, balloon experiments were frequently performed to study the atmospheric profile of ozone. In 1987 it was carried out 76 balloon observations. Helium was used in the balloons, which could reach an altitude of approximately 30 km (10 hPa pressure). It was measured ozone, temperature, altitude and wind. Observations were made every minute after launch, and the ozone concentration was plotted as a function of height. The balloon observations from the South Pole are presented in Figures 4.5 and 4.6.

[1] The polar vortex is characterized by stratospheric air moving in circular motion, with an area of relatively still air in its center.

From Figure 4.5 it can be seen that the ozone values varied between 250 and 300 DU for a large part of the year. In September the large ozone loss started and the ozone hole lasted until the end of November. The average ozone value for September was 21% below normal, for October 50% and for November 44% below normal. The average ozone value for the 11 balloon observations in October was 140 DU.

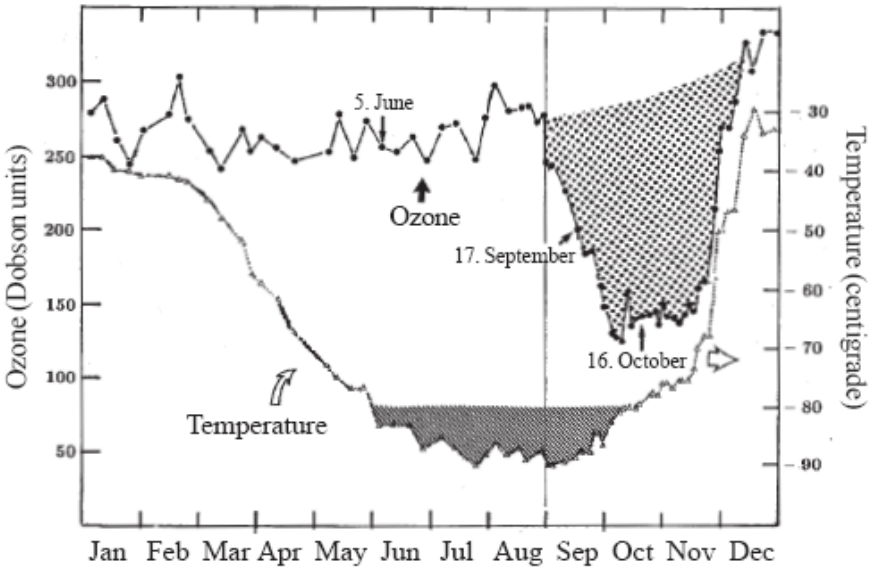

Figure 4.5: *Antarctic ozone values in 1987. The upper curve represents total ozone (in DU, left axis), whereas the dotted region indicates the ozone hole. The lower curve shows the mean temperature at altitude 14 to 19 km (given in ℃, right axis). The grey area represents the time period when the temperature was below -80℃, i.e. from the beginning of June until the end of October. Three days are marked in the Figure and the height profiles for these days are represented in Figure 4.6. (Source: NOAA Report ERL ARL-15, 1988).*

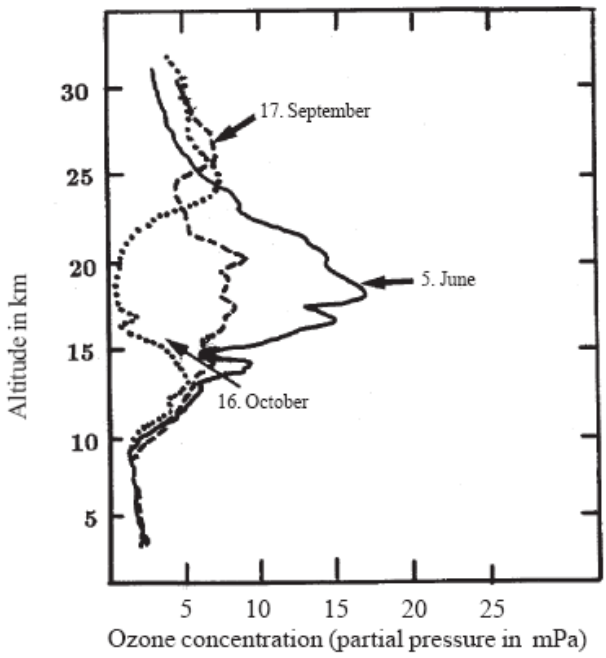

Figure 4.6: *The vertical distribution of ozone at the South Pole three days in 1987. In early June the ozone situation was quite normal with a maximum in the region 15 to 20 km. On September 17th the ozone destruction had started (compare to Figure 4.5). The curve labeled October 16th shows the vertical ozone distribution during a period with maximum depth of the ozone hole. Note that the ozone loss is restricted to a certain altitude region (Source: NOAA Report ERL ARL-15, 1988).*

In the balloon experiments the temperature was also observed. The mean temperature at altitudes 14 to 19 km (i.e. 100 to 50 hPa pressure) is given by the lower curve in Figure 4.5. The lowest temperatures are usually found between 15 to 25 km altitude: above 20 km in the wintertime and below 20 km in the summertime. As can be seen from Figure 4.5 the temperature is below -80°C several months **before** the ozone hole forms. However, this is a period with polar night. In Antarctica the solar light returns in August-September (indicated by the vertical line in Figure 4.5).

The data presented in Figures 4.5 and 4.6 clearly demonstrate the formation and the behaviour of what we call "The Antarctic Ozone Hole". It is a transient thinning of the ozone layer during the Antarctic spring months September, October and November. Figure 4.6 indicates that the ozone loss is restricted to the altitude region from 12 to 20 km. In this region almost all ozone is broken down.

> The Figures above clearly demonstrate two parameters that are needed for the formation of the Antarctic ozone hole:
> **sunlight** and **cold stratosphere**.
> As will be described in the next chapter a third parameter is needed: active radicals such as **chlorine**.

The first ozone observations made in Antarctica demonstrated that the spring values (from September to November) always have been fairly low until the Polar Vortex collapses. However, the ozone spring values decreased continuously through the 1970s, 1980s and 1990s. In recent years ozone destruction similar to the episode described for 1987 occurs every year. However, the depth of the ozone hole, the duration of the depletion and the extent of the area included can vary from year to year. These variations are mainly related to meteorological conditions.

Extent. During the last decade the ozone hole has reached an extent of more than 20 million km^2 (as a comparison the size of US is about 9 million km^2). 2006 was a record year, where the ozone hole covered an area of about 27 million km^2 (see Figure 4.7, upper panel). The ozone hole in 2008 was larger than 2007 but not as large as 2006.

Duration. The duration of the ozone depletion is closely connected to the Polar Vortex. A parameter for "duration" is the number of days where the depletion covers an area of more than 15 million km^2. The duration can be up to 100 days. Again 2006 was a year with a very long lasting depletion.

Depth. The lowest ozone values observed are around 100 DU. Such a low value implies that the ozone layer is approximately 65% below "normal". The depths of the ozone hole for the last ten years are visualized in Figure 4.7 (lower panel).

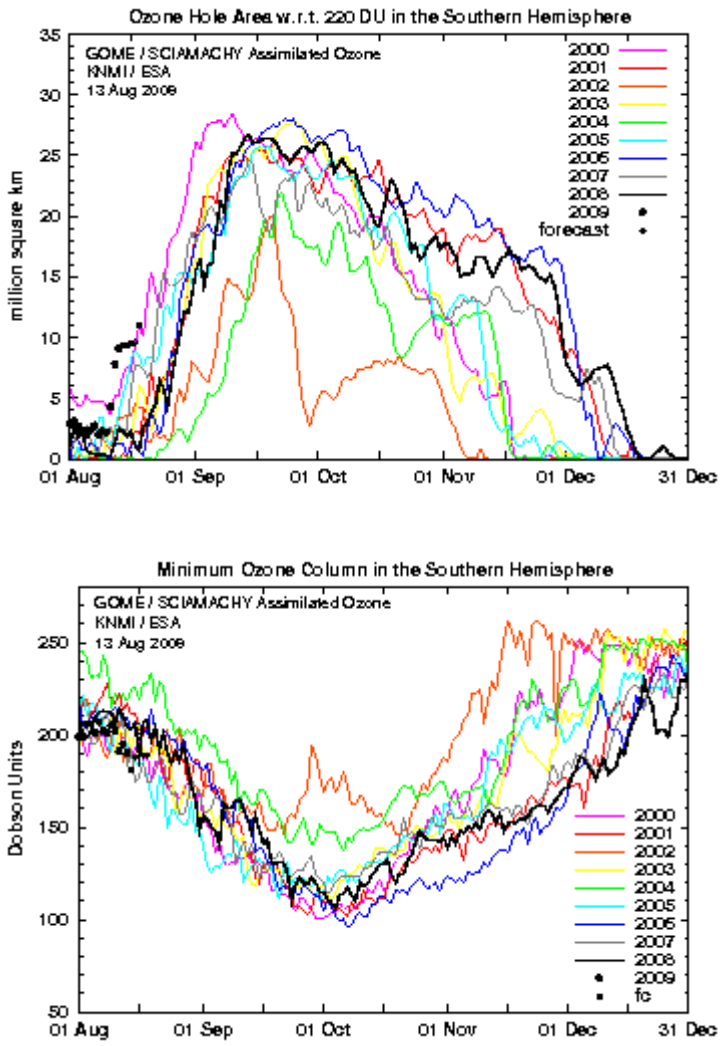

Figure 4.7: *The Arctic ozone hole from 2000 to 2009. Upper panel shows the extent and duration of the ozone hole, whereas the lower panel shows the depth (Source: http://www.temis.nl/protocols/o3hole2/)*

Chapter 5

Ozone formation and destruction

In this chapter we will study the chemical processes for formation and destruction of ozone in the atmosphere. For most processes photochemistry plays an important role for the formation as well as destruction of ozone. We differ between the formation of ozone at high altitudes (in the stratosphere) and the processes responsible for ozone formation in the troposphere.

5.1. Formation and destruction by light

The atmosphere consists mainly of nitrogen and oxygen (78% nitrogen and 21% oxygen). The main part of the oxygen is in the molecular form O_2, but there is also some atomic oxygen (O) and ozone (O_3). The ozone is formed when UV-radiation from the sun (with energy $h\nu$ penetrates the atmosphere. This was briefly described in Chapter 2.

Sidney Chapman was the first person who tried to give a theoretical explanation for the formation and destruction of atmospheric ozone. In 1930 he suggested a photochemical oxygen balance based on the following reactions:

$O_2 + h\nu \Rightarrow O + O$	(O_3 formation: $\lambda \leq 242.4$ nm)	(5.1)
$O + O_2 + M \Rightarrow O_3 + M$		(5.2)
$O_3 + h\nu \Rightarrow O + O_2$	(O_3 dissociation: $\lambda \leq 320$ nm)	(5.3)
$O + O_3 \Rightarrow 2O_2$		(5.4)
$O + O + M \Rightarrow O_2 + M$		(5.5)

As briefly explained in Chapter 2.3 the key process to ozone formation is the splitting of the oxygen molecule (equation (5.1)). This implies that the bond in the oxygen molecule (O - O) must be broken. It requires energy of 5.115 eV to split the oxygen molecule, meaning that the solar radiation must have wavelength of 242.4 nm or shorter.

UV-radiation with wavelengths below 242.4 nm is absorbed high up in the atmosphere (see Figure 5.1), normally at altitudes above 40 km. The formation of ozone depends upon the concentration of oxygen and the intensity of these high-energy photons. Since the formation of ozone depends on the solar intensity the formation process is most

efficient in the tropical region - and of course on the side of the Earth pointing towards the sun.

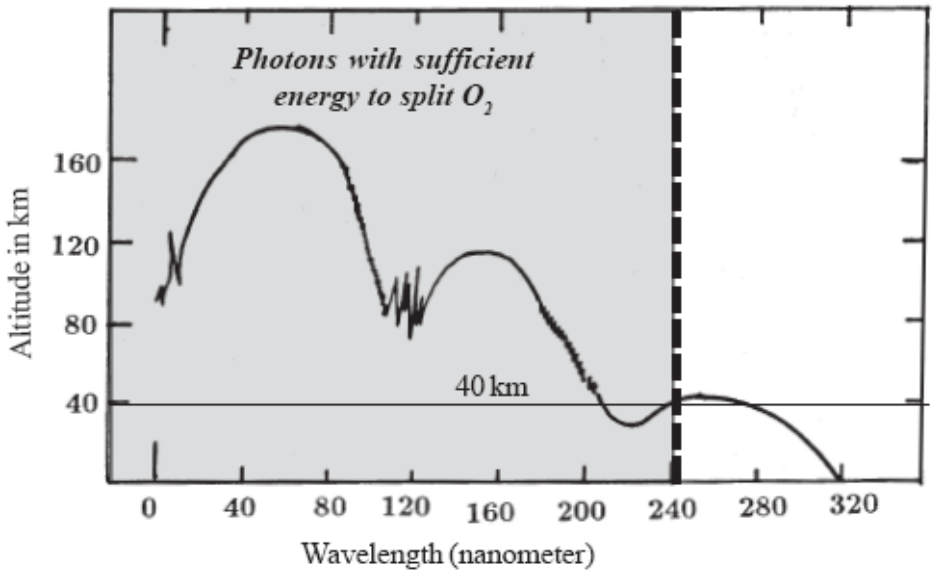

Figure 5.1: *Altitude dependent absorption of UV-radiation in the atmosphere. The curve indicates where the solar radiation with a certain wavelength is reduced to 37% of the value at the top of the atmosphere. Radiation within the grey area has sufficient energy to split the oxygen molecule.*

If the ozone layer had been stationary it would be thickest in the tropical region and decrease gradually towards the two poles. In previous chapters we have seen that the global ozone distribution has a different pattern due to the transport of ozone by the wind systems. An interesting question arises: How long does it take to produce the ozone layer?

The reaction rate for ozone formation depends on the concentrations of oxygen and ozone, their absorption spectra and the amount of radiation with sufficient energy to split the oxygen atom. At altitudes where the ozone production is most effective, i.e. in the stratosphere around equator at noon, it would only take a few weeks to produce the entire ozone layer (can you verify this from exercise 4 on page 72?).

The lifetime of an ozone molecule will also vary considerably depending on its location. The solar radiation will rapidly destruct the ozone molecule at an altitude of 40 km, but the lifetime can be several days or weeks at lower altitudes and/or higher latitudes.

5.2. Ozone destruction

Until the 1960s it was more or less accepted that Chapman's equations (5.1 to 5.5) could explain the balance between formation and destruction of ozone in the atmosphere.

Eventually it was realised that the destruction reaction (5.4) was too slow compared to the formation rate. It was concluded that other processes had to contribute to the destruction of ozone.

Around 1950 M. Nicolet and D.R. Bates demonstrated that water radicals, such as OH and HO_2 could influence the ozone layer. Today we know that a number of reactive radicals may destruct ozone catalytically. In these reactions the radicals take an active part in the destruction, but they are regenerated in the process and can initiate a series of cycles.

5.2.1. Catalytic gas phase chemistry

During the last decades there has been much attention to manmade compounds that can reach the stratosphere and act as ozone destructing radicals. The radicals may disturb the existing balance between formation and destruction of ozone and contribute to a depletion of the ozone layer. The following reactions can take place:

$$R + O_3 \Rightarrow RO + O_2 \qquad (5.6)$$
$$RO + O \Rightarrow R + O_2 \qquad (5.7)$$

The net result:

$$O_3 + O \Rightarrow O_2 + O_2$$

The radical R can e.g. be nitric oxide (NO), a halogen radical (Cl or Br) or a water radical (H, OH, HO_2).

Altogether the catalytic destruction via reactive radicals gives the same final result as the Chapman reaction (5.4). The radicals that have largest impact on the global ozone level are those from nitrogen, water and chlorine compounds.

5.2.1.1. Destruction by nitrogen oxides

It was proposed by Paul Crutzen that nitrogen oxides could be important contributors to the destruction of ozone. Two nitrogen oxides, NO and NO_2, can either destruct ozone directly or consume atomic oxygen and thereby prevent ozone formation. The two most important processes are:

$$NO + O_3 \Rightarrow NO_2 + O_2$$
$$NO_2 + O \Rightarrow NO + O_2$$

In the reactions ozone is destroyed whereas the nitrogen radicals are regenerated and can start over again with a new ozone molecule. The process can be stopped by the following reaction:

$$NO_2 + OH + M \Rightarrow M + HNO_3$$

The reaction with hydroxyl (OH) results in the formation of nitric acid (HNO_3), which is washed out of the atmosphere by the rain. The important OH radical can break the reaction loop of NO.

Manmade sources such as fertilizers and combustion engines contribute to an increase in the tropospheric NO concentration. In nature the NO radicals are formed from N_2O, which is formed from bacteria in water and the ground. Most of the N_2O will be washed out with the rain, but a certain fraction will react with excited oxygen and form NO radicals according to the following reaction scheme:

$$N_2O + O(^1D) \Rightarrow 2NO$$

5.2.1.2. Destruction by water radicals - HO_x

A group of radicals that are quite important for the ozone depletion originate from water. The radicals are the H-atom, the OH-radical and HO_2. We will not describe all the reactions involving these radicals, but only mention that the OH-radical can be formed when singlet oxygen reacts with water:

$$H_2O + O(^1D) \Rightarrow 2OH$$

Also a number of other photochemical reactions, for example reactions with methane, can produce HO_x radicals. A reservoir for HO_x is hydrogen peroxide H_2O_2, which in turn yield OH-radicals by photolysis. As explained in the previous chapter reactions between OH and NO_2 are important in the trapping of the OH-radicals, and also for breaking the reaction loop of NO.

5.2.1.3. Destruction by halogens

During the last decades there has been much focus on anthropogenic compounds that are capable of perturbing atmospheric ozone levels. Chlorine (Cl), released from chloro-fluorocarbons (CFCs) and bromine (Br), released from halons, are two of the most important groups of chemicals associated with ozone depletion. For chlorine the depletion takes place according to the following reactions:

$$Cl + O_3 \Rightarrow ClO + O_2$$
$$ClO + O \Rightarrow Cl + O_2$$

The halogen radicals may originate from natural sources, for example methylchloride (CH_3Cl), which is released in large quantities from the ocean. Chlorine is also released from volcano eruptions. However, most of these compounds are efficiently removed from

the atmosphere owing to high solubility. Thus, the majority of chlorine found in the atmosphere today originates from breakdown of manufactured chlorofluorcarbons (CFCs).

Description of halocarbons

In 1974 Mario Molina and Sherwood Rowland published an article in Nature (volume 249, 1974) suggesting that the CFC-gases are important sources for the chlorine radicals:

Chlorofluoromethanes are being added to the environment in steadily increasing amounts. These compounds are chemically inert and may remain in the atmosphere for 40 - 150 years, and concentrations can be expected to reach 10 to 30 times present levels. Photodissociation of the chlorfluoromethanes in the stratosphere produces significant amounts of chlorine atoms, and leads to the destruction of atmospheric ozone.

Crutzen, Molina and Rowland were awarded the 1995 Nobel Prize in Chemistry for their work on this problem.

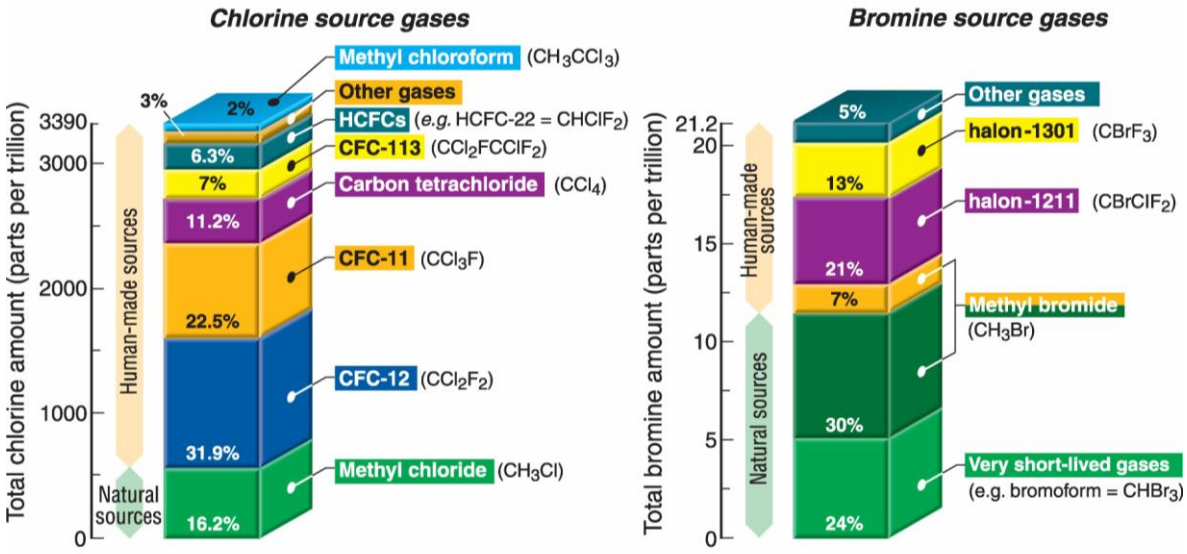

Figure 5.2: *Stratospheric source gases. The columns show how the principal chlorine and bromine source gases contribute to the total amounts of chlorine and bromine as measured in 2004. Note the large difference in vertical scales (Source: Scientific Assessment of Ozone Depletion: 2006)*

Halocarbons are compounds where one or more carbon atoms are bound to fluorine (F), chlorine (Cl) and/or bromine (Br). The most important gases are presented in Figure 5.2. ***CFCs*** are gases containing Cl, whereas ***halons*** contain Br.

Traditionally we have used CFCs and halons for several purposes. Halons have primarily been used in fire extinguishers, whereas CFCs have been used extensively in spray cans, air conditioners, refrigerators, and cleaning solvents. Near the Earth's surface, CFCs are relatively harmless and do not react with any material, including human skin. However, the very quality that made them seem so safe, their stability, is what makes them so harmful to the ozone layer. Most of the CFCs and halons have atmospheric residence times of about 50 to hundred years.

The release of CFC-gases started around 1950 and increased drastically up to the 1980s. However, in 1987 a number of the countries signed a treaty with the aim of phasing out and finally stop the release of ozone depleting substances (**The Montreal Protocol**). Since 1987 the Montreal Protocol has undergone several revisions. Due to its widespread adoption and implementation it has been hailed as an example of exceptional good international cooperation.

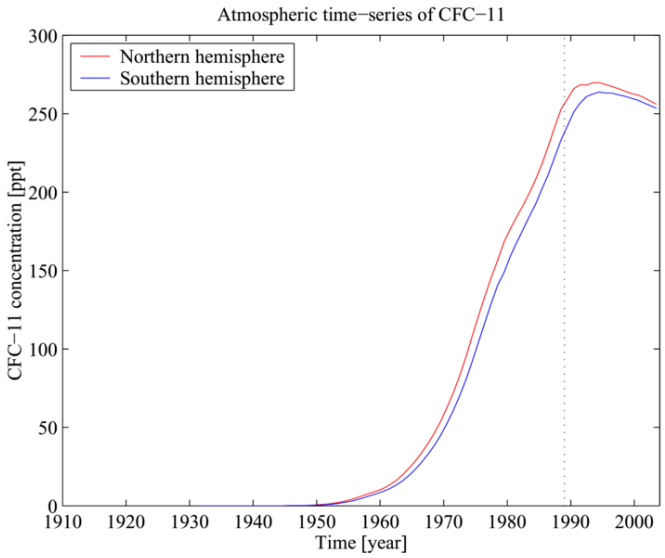

Figure 5.3: *Time-series of atmospheric concentration of CFC-11 (Walker et al., 2000). Along the vertical axis is given the mixture ratio (parts per trillion, i.e. per 10^{12}).*

5.3. Heterogeneous chlorine chemistry and ozone holes

When the CFC-molecules have reached the stratosphere the solar radiation gets more intense and will break down the molecules with the formation of less stable products such as $ClONO_2$ and HCl. These reservoir molecules are not directly involved in ozone destruction, but they have the potential of releasing active chlorine components. The following five heterogeneous reactions will typically occur *in the presence of aerosols or ice crystals:*

$$HCl + ClONO_2 \Rightarrow HNO_3 + Cl_2 \quad (5.8)$$
$$ClONO_2 + H_2O \Rightarrow HNO_3 + HOCl \quad (5.9)$$
$$HCl + HOCl \Rightarrow H_2O + Cl_2 \quad (5.10)$$
$$N_2O_5 + HCl \Rightarrow HNO_3 + ClNO_2 \quad (5.11)$$
$$N_2O_5 + H_2O \Rightarrow 2\ HNO_3 \quad (5.12)$$

The chlorine molecules (Cl_2) are not very reactive. However, they can be split by the sun and form reactive chlorine radicals. The HNO_3 molecule can influence the ozone balance in two different ways: it can keep the reactive catalytic OH molecules out of the ozone destruction reactions and thereby prevent ozone depletion. On the other hand HNO_3 can bind NO_2 and prevent the completion of the ozone destruction cycles described in 5.2.1.

Within the polar vortex over Antarctica it is a rapid destruction of ozone in September each year. This process can be explained by heterogeneous chemistry. The chemical reactions (5.8) to (5.12) are slow processes in a pure gas phase, but they may take place quickly and efficient on stratospheric clouds of ice particles called PSCs or "*Polar Stratospheric Clouds"*. The particles in the clouds act as reaction sites where chlorine can be released from the atmospheric chlorine reservoirs HCl and $ClONO_2$ (see reactions (5.8) and (5.9)). The chlorine is transformed from an inactive form to the more active forms Cl_2 and HOCl.

In summary the following processes occur over Antarctica:

1. **The ozone layer above Antarctica** exhibits a time dependent depletion (September, October, November) of about 40 - 50%. Ordinary gas-phase photochemistry cannot explain such a rapid and large depletion.

2. **The destruction takes mainly place at altitudes from 12 to 22 km.** Sometimes the ozone depletion in this region can be as large as 90 %.

3. **The ozone destruction takes place when the temperature at altitudes 12 - 22 km is very low** (lower than -80°C). Under these cold conditions PSCs are formed.

4. **The depletion takes place when the solar light returns to the area** (see Figure 4.5). This implies that photochemical reactions are important.

5. **The polar vortex** prevents transport of ozone rich air from lower latitudes.

5.3.1. PSCs and Mother-of-Pearl clouds

In the atmosphere there are three major types of ice clouds or surfaces that are believed to contribute to heterogeneous reactions: (1) Type I polar stratospheric clouds (PSCs), which are composed of nitric acid trihydrate ($HNO_3 \bullet 3H_2O$), formed at about -78°C; (2) Type II PSCs which consist of relatively pure water crystals, formed at about -85°C; and (3) sulfuric acid aerosols, generally in liquid phase, composed of 60–80% H_2SO_4 and 40–20% H_2O. While PSCs are formed primarily in the cold winter stratosphere at high latitudes, sulphuric acid aerosols are present year round at all latitudes and may influence stratospheric chemistry on a global basis.

The stratospheric ozone is destructed when the O_3 reacts with chlorine (Cl) and form ClO (see chapter 5.2.1.3). Next, the following reactions can take place:

$$ClO + ClO + M \Rightarrow Cl_2O_2 + M \quad (5.13)$$
$$Cl_2O_2 + h\nu \Rightarrow Cl + ClO_2 \quad (5.14)$$
$$ClO_2 + M \Rightarrow Cl + O_2 + M \quad (5.15)$$

In reactions (5.14) and (5.15) reactive chlorine (Cl) is formed. The destruction of ozone is usually determined by the concentration of ClO-dimers (Cl_2O_2). The ozone destructing cycle can be stopped by other atmospheric compounds, for example NO_2:

$$ClO + NO_2 + M \Rightarrow ClONO_2 + M$$

The NO_2 molecules can also form HNO_3, which is condensed in the PSCs. In this way NO_2 is removed from the gas phase and will prevent the formation of $ClONO_2$ and thereby prevent the destruction of reactive ClO. Altogether there are several competing processes and complex mechanisms that influence formation and destruction of stratospheric ozone.

If we go back to Figure 4.5 we can see that the temperature in Antarctica was below -80°C already in June. However, no ozone destruction took place before the beginning of September. At this time the sun returned and made it possible to form the reactive chlorine radicals from the splitting of Cl_2.

As seen in Figure 5.4 the temperatures are generally not as low in the Arctic as in Antarctica, partly due to a weaker and less stable vortex. Thus, the magnitude of PSC formation is smaller in the Arctic. PSC I particles, however, also called nacreous or mother-of-pearl clouds, are formed during cold and favourable conditions and might initiate heterogeneous ozone destruction at latitudes down to 60°N (e.g. in Oslo). It is interesting to note that a correlation between ozone destruction and mother-of-pearl clouds in Norway was observed by K. Langlo more than 60 years ago. At that time they had no good explanations for these findings.

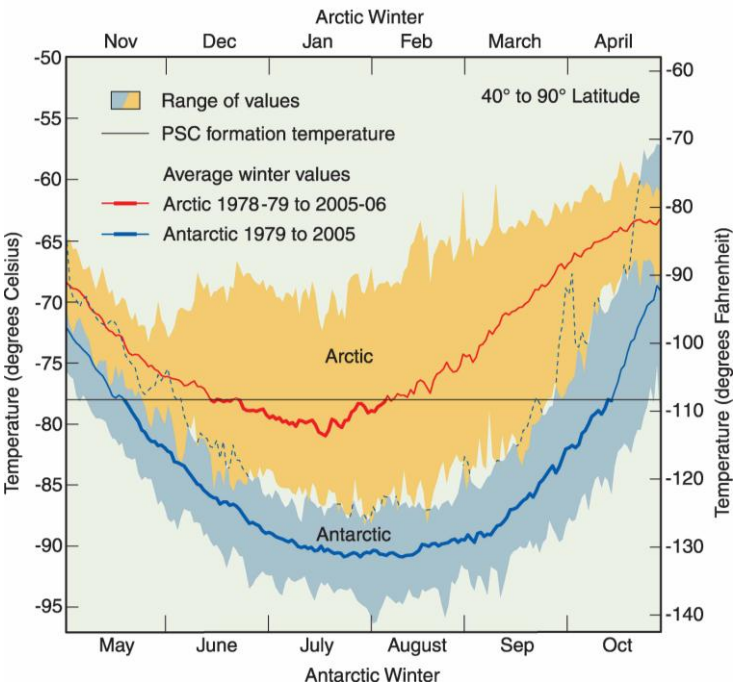

Figure 5.4: *Stratospheric air temperature in Arctic and Antarctica. Average mini-mum values over Antarctica are as low as –90℃ in July and August in a typical year. Over the Arctic, average minimum temperature values are near –80℃ in January and February. PSCs are formed when the temperature fall below –78℃ (Source: Scientific Assessment of Ozone Depletion: 2006)*

5.4. Impact of volcano eruptions

Aerosols of sulphuric acid and water are always present in the atmosphere. Small droplets are formed when carbonyl sulphide (OCS) from the ocean is oxidized. This is a natural sulphur component that has sufficient lifetime to survive a slow transport to the stratosphere. In a volcano eruption the amount of aerosol can increase drastically. H_2S_2, which is released, is oxidized and form SO_2. In the course of a few months the SO_2 is transformed into H_2SO_4 vapour, which in turn is condensed on aerosols.

The volcano eruption must be very powerful to enable dust and gas to penetrate the tropospause and reach the stratosphere. This will not happen for most eruptions but in the course of the last decades we have had two powerful eruptions. The first one occurred in April 1982 from the volcano "***El Chichon***", Mexico, at latitude of 18°N. The other one was "***Mt. Pinatubo***" on the Philippines in June 1991.

Figure 5.5 shows aerosol observations at the Mauna Loa observatory on Hawaii. The measurements represent the altitude region from 16 to 33 km during the time period from 1980 to 1995.

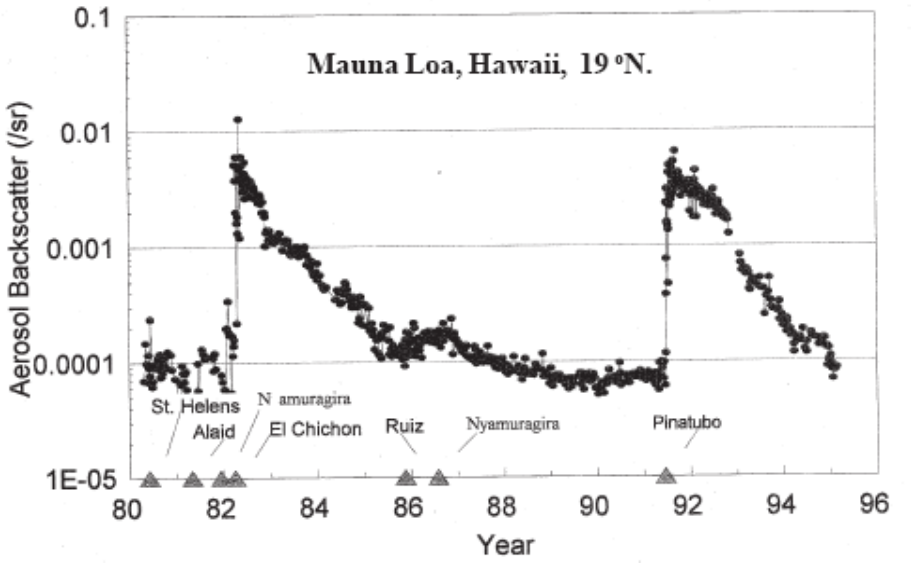

Figure 5.5: *The Mauna Loa Ruby Lidar shows the amount of aerososl above Hawaii at the altitude 15.8 to 33 km. The dates for a number of volcano eruptions are marked along the horizontal axis. The eruptions from El Chichon and Mt. Pinatubo increased the aerosol concentrations considerably.*

Figure 5.5 clearly demonstrates that the stratospheric aerosol concentration increased dramatically after the two volcanoes. After strong eruptions the emitted dust and particles will initially circulate around the Earth at the same latitude as the volcano. Subsequently, the aerosols will dispersed and reach other latitudes. Consequently, it might take some time before a volcano eruption in the tropical regions will influence the ozone layer at higher latitudes.

In Figure 5.6 the running annual ozone mean over Oslo is presented. In 1983, 1992 and 1993 very low ozone values were observed. A comparison of the two Figures 5.5 and 5.6 suggests that the amount of aerosols in the stratosphere is important for the destruction of atmospheric ozone. Most likely heterogeneous destruction based on sulphuric acid aerosols and chlorine radicals plays a significant role.

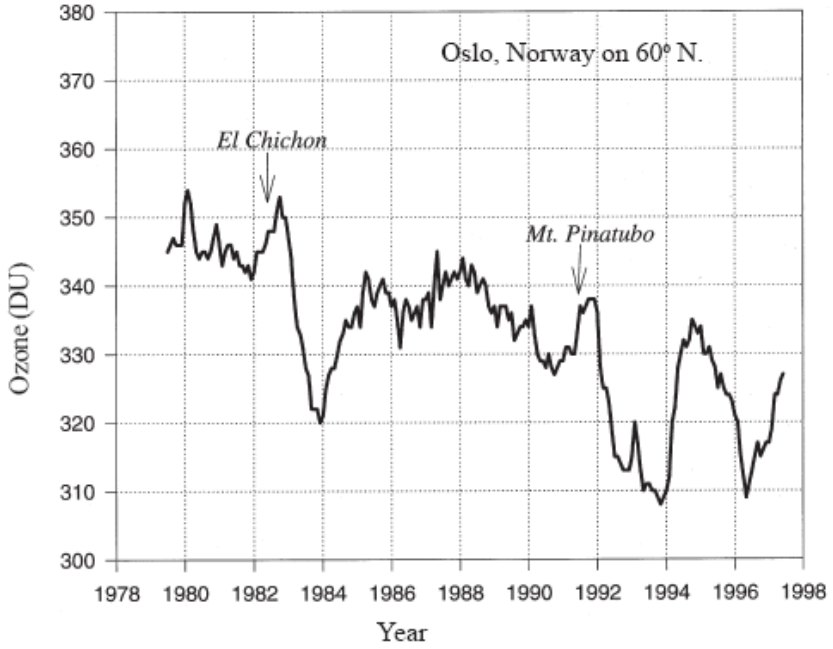

Figure 5.6: *Running annual ozone mean over Oslo (latitude of 60 °N) for the period 1978 to 1997. The running annual mean is the average of 12 months, displaced forward in time with a step of one month. The eruptions of El Chichon and Mt. Pinatubo are marked.*

5.5. Impact of climate change on ozone

Changes in Earth's climate might affect the future ozone layer. Stratospheric ozone is influenced by changes in temperatures and winds in the stratosphere. For example, lower temperatures and stronger polar winds could both affect the extent and severity of winter polar ozone depletion. While the Earth's surface is expected to warm in response to the net positive radiative forcing from greenhouse gas increases, the stratosphere is expected to cool. A cooler stratosphere would extend the time period over which polar stratospheric clouds (PSCs) are present in Polar regions and, as a result, might increase winter ozone depletion. In the upper stratosphere at altitudes above PSC formation regions, a cooler stratosphere is expected to increase ozone amounts and, hence, hasten recovery, because lower temperatures favour ozone production over loss (the ozone destructing processes become less effective).

It should be noted that there are other important links between ozone and climate changes. First, ozone is a greenhouse gas that absorbs infrared radiation emitted by the

Earth's surface, effectively trapping heat in the atmosphere. Thus, a reduced ozone layer will reduce the warming of the Earth. On the other hand there has been an increase in tropospheric ozone during the last decades. The warming due to tropospheric ozone increase is currently larger than the cooling associated with stratospheric ozone depletion.

Another important link between ozone depletion and climate changes is related to the halocarbons and hydrofluorcarbons (HFCs). HFCs are substitute gases that have been introduced to replace the ozone destruction halogens. The HFCs are not harmful for the ozone layer, but instead they are effective greenhouse gases. Also the traditional halocarbons are greenhouse gases that contributed to increased surface temperature.

5.6. When is the ozone layer expected to recover?

Ozone depletion caused by human-produced chlorine and bromine gases is expected to gradually disappear around the middle of this century as the abundances of these gases decline in the stratosphere. The decline in *stratospheric chlorine* will follow the reductions in emissions that are expected to continue under the provisions of the Montreal Protocol.

A decline of several halogen gases has already been observed. However, natural chemical and transport processes limit the rate at which halogen gases are removed from the stratosphere. The atmospheric life-times of the halogens are up to 100 years, but CFC-12 (with its 100-year lifetime) will require about 200 to 300 years before it is removed from the atmosphere. At midlatitudes, effective stratospheric chlorine is expected to reach pre-1980 values around 2050.

Computer models of the atmosphere are used to assess past changes in the global ozone distribution and to project future changes. Two important features are

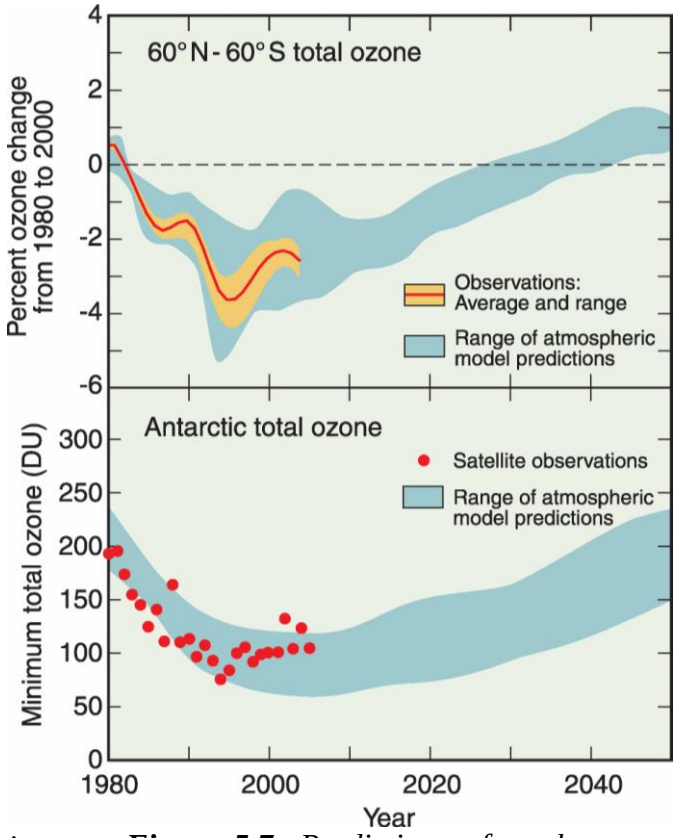

Figure 5.7: *Predictions of total ozone recovery. Observed values of midlatitude (top panel) and September-October values over Antarctica (bottom panel). (Source: Scientific Assessment of Ozone Depletion: 2006)*

studied in the models: total ozone averages between 60°N and 60°S, and minimum ozone values in the Antarctic "ozone hole". The model projections (shown in Figure 5.7) indicate that for 60°N-60°S total ozone, the recovery is expected to occur by the middle of this century. Some of the models indicate that the recovery might even happen before mid-century.

For Antarctica full recovery could occur by mid-century but some models show later recovery, between 2060 and 2070. It is also predicted that declines in stratospheric chlorine amounts will occur later over Antarctica than at lower latitudes because air in the Antarctic stratosphere is "older" than air found at lower latitudes. As a result, reductions in halogen loading to pre-1980 values will occur 10-15 years later in the Antarctic stratosphere than in the midlatitude stratosphere.

5.6. Conclusion

In this chapter we have discussed the different reactions that lead to the formation of atmospheric ozone as well as processes that are responsible for the destruction of ozone. It must be a balance between the formation and destruction, which yield a stable ozone layer. Because of meteorological variability we will normally observe large variations from this stable position. During the 80 years period with ozone measurements we have had both periods with increasing as well as decreasing amount of ozone.

The ozone depletion during the last three decades has been ascribed to the release of manmade CFC-gases. Already in 1974 Rowland and Molina suggested that this chlorine source could alter the balance of the ozone layer. However, their models were based on ordinary gas chemistry. Several years later the theory of heterogeneous chemistry was proposed to explain the large ozone loss in Antarctica.

Most likely we will have an ozone hole in Antarctica every spring for several decades, until the chlorine concentration is back to normal. In the Arctic we might see an increase in the number of smaller ozone holes in the future due decreased stratospheric temperature from climate changes. However, since the stability of the Arctic Polar vortex is different from the Antarctic, the increase in surface UV-radiation is far less dramatic.

It is also reasonable to assume that large and powerful volcano eruptions will enhance the ozone depletion as long as the stratospheric chlorine concentration is high, but the strength and frequency of future eruptions are impossible to predict.

Chapter 6

UV-radiation through the ozone layer

The ozone layer acts as a filter for the UV-radiation from the sun. It is mainly UV-radiation with short wavelengths (UVC and UVB, see Table 1.2) that is absorbed. UVA-radiation is to a small extent influenced by ozone. This can be seen from the absorption spectrum in Figure 1.3.

UV-radiation can cause both positive and negative biological effects. UVB, i.e. radiation in the wavelength region from 280 nm to 320 nm, have several negative effects on humans and environment and is sometimes called "*damaging UV-radiation"*.

In this chapter we will describe the UV-radiation that reaches the ground and affects life on Earth. We will define some common terms, such as "UV-dose". This is not a simple definition because all biological effects vary with the wavelength of the radiation. For example, there are two different wavelength regions that are responsible for sunburn and ageing of the skin.

6.1. Absorption spectra

The "**absorption spectrum**" is very important in the field of photobiology. In Figure 1.3 the absorption spectrum for ozone is shown. The eye has a totally different spectrum. We have certain molecules (chromophores) in the retina that absorb different regions of the visible light. The combined response from these three chromophores makes it possible to register colours.

When a compound is irradiated it is also possible to use the characteristic absorption spectrum to identify the compound and to determine its concentration. In Figure 6.1 the absorption spectra for proteins and DNA are given. As seen from the figure these molecules absorbs mainly in the UVC and UVB regions. The absorption in the UVA-region is almost absent.

In order to determine absorption spectra (like those in Figure 6.1) experiments with monochromatic light are performed. By measuring light transmittance for all relevant wavelengths the absorption spectrum can be derived.

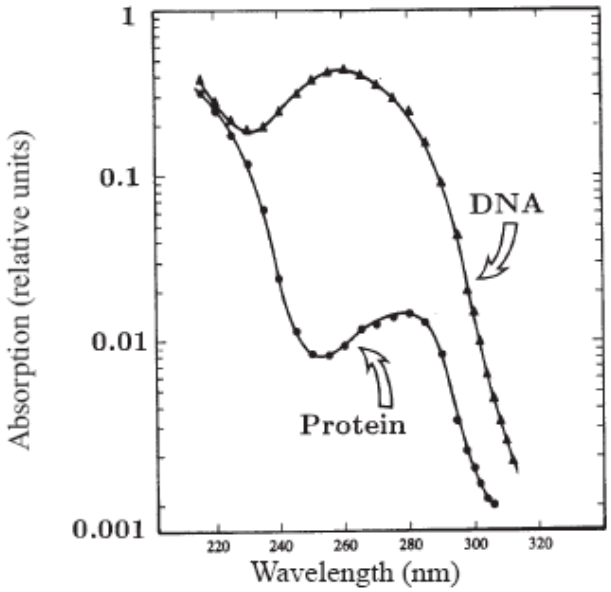

Figure 6.1: *Absorption spectra for proteins and DNA. The absorption spectrum shows the amount of radiation absorbed as a function of wavelength. The absorption is given in relative units. Note that the scale is logarithmic because of the large differences in absorption between UVB and UVA.*

6.2. Action spectra

When UV-radiation hits a biological system several processes may be initiated. Some of them are considered as positive, whereas others are negative. For example UV may change the skin by forming pigments - a tanning which normally is considered as positive. Burning of the skin, however, is painful and damaging. We also know a number of other processes that are influenced by UV, i.e. the immune system and vitamin D production.

The efficiency of the radiation depends on the wavelength. Thus, in the same way as the absorption varies with wavelength, the biological effect will also vary as a function of wavelength. The response spectrum is called the "**action spectrum**".

Figure 6.2 illustrates the action spectra for three different biological effects: skin cancer for a mouse, erythema (redness of the skin) for humans, and mutation of cells in the basal layer of the skin. Information about the action spectra can give us valuable information about the influence of UV-radiation on biological systems.

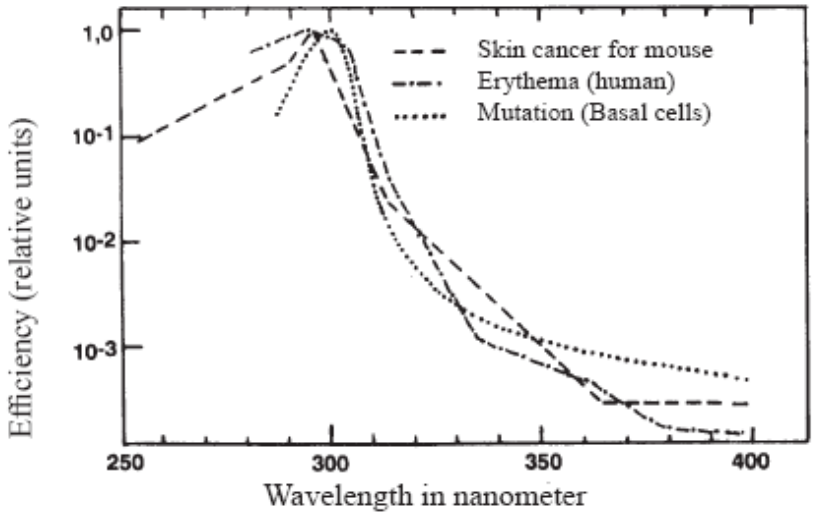

Figure 6.2: *Action spectra for a) skin cancer in mouse (non-melanoma skin cancer), b) erythema, and c) mutations of cells in the basal cell layer of the skin. Along the horizontal axis is wavelength and along the vertical axis is the relative efficiency (the maximum is set equal to 1.0 for all three effects).*

6.3. Dose rate and UV-dose

Processes that are influenced by the solar radiation will normally depend on the dose, usually called "**UV-dose**" if UV radiation triggers the effect. In order to define a UV-dose we have to take the action spectrum and the solar intensity into account. If a process is initiated by radiation in the wavelength region 295 to 330, nothing happens if the system is irradiated by visible light in the region 400 to 800 nm.

First we define the term **"efficiency spectrum**", which is the product of the solar spectrum $I(\lambda)$ and the action spectrum $A(\lambda)$:

$$E(\lambda) = I(\lambda) \cdot A(\lambda)$$

For light sources other than the sun, e.g. artificial UV-lamps, the spectrum of the lamp or the different light sources represent $I(\lambda)$.

Another useful quantity is the **"dose rate"**. It is defined as the integrated efficiency spectrum:

$$\frac{dD}{dt} = \int_{\lambda} I(\lambda) A(\lambda) d\lambda \qquad (6.1)$$

If the biological effect is caused by UV-radiation from the sun, the integral in (6.1) will cover the wavelength region from 290 nm to 400 nm.

The solar spectrum depends on a number of different parameters such as the thickness of the ozone layer, the cloud cover and the solar zenith angle. Thus, the solar spectrum will vary as a function of time, date and location (latitude, longitude and altitude). In Figure 6.3 the solar spectra measured in Oslo in July at 1pm and 5pm are shown.

When we specify the solar radiation as a function of both wavelength and time, I(λ,t), the **UV-dose** for the specified time period is defined as:

$$D = \int_0^t \int_{290}^{400} I(\lambda,t)A(\lambda)d\lambda dt \qquad (6.2)$$

The time interval can be chosen as desired, e.g. an hour, a day or a year. The wavelength region typically covers 290 nm to 400 nm. The action spectrum *A(λ)* depends on the biological process in question.

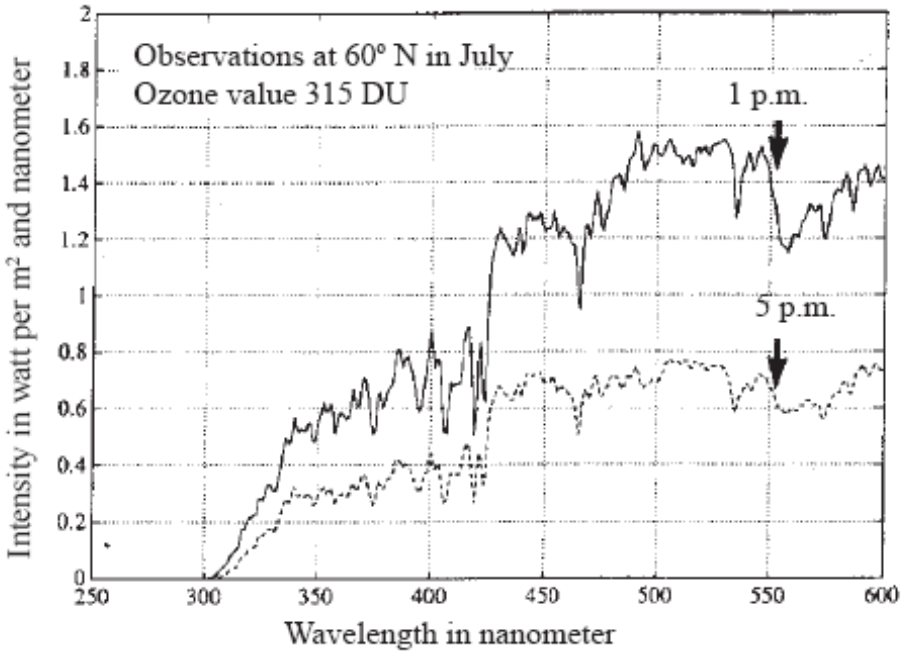

Figure 6.3: *The solar spectrum at the ground at 1pm and 5pm. When the sun is low the path through the atmosphere is long and a large fraction of the radiation is absorbed and scattered. The ozone value is the same in both spectra (315 DU).*

6.3.1. CIE and Setlow action spectra

In most situations we are concerned about UV effects causing sun burn or skin cancer. Different action spectra have been used throughout the years to describe the negative effects of UV exposure. Since DNA is of major importance for cell damage, the absorption spectrum for DNA was originally used as a relevant action spectrum when calculating UV-doses.

In Figure 6.2 the action spectra for three different processes are presented. These spectra have quite similar shapes, with a much higher efficiency for UVB-radiation compared to UVA (note the logarithmic scale in Figure 6.2). It has been constructed an idealized action spectrum which roughly describes formation of erythema in human skin. The spectrum was suggested by CIE (*«Commission Internationale de l`Éclaire»)* and is therefore called the **"CIE-spectrum"**. Today this is the most commonly used spectrum for calculations of UV-doses.

The CIE-spectrum (shown in Figure 6.4) covers the whole UV-region and is represented by three straight lines that easily can be described mathematically. The expressions are summarized in the table below:

Wavelength (nm)	**Efficiency A(λ)**
0 – 298	1.0
299 – 328	exp(0.2164(298-λ))
329 – 400	exp(0.0345(139-λ))

UVA will to a small extent cause erythema or sun burn. Still, the effect of UVA exposure has received much attention after a publication from Richard B. Setlow and co-workers[2] in 1993. They performed lots of experiments where small fish, Xiphororus, were exposed to radiation of different wavelengths. The experiments showed that the fish efficiently developed skin cancer (melanomas) after UVA exposure. The action spectrum, called the **"Setlow-spectrum"** is shown in Figure 6.4.

If the molecular mechanisms for the formation of melanoma in fish are similar to the mechanisms in humans, it can be assumed that the Setlow-spectrum is a representative action spectrum for the formation of malignant melanoma (the most dangerous form of skin cancer). It is believed that UVA produces reactive melanin radicals that can cause melanoma[3]. This would imply that UVA is far more important for melanoma formation than previously assumed.

---

[2] R.B. Setlow, E. Grist, K. Thompson and A.D. Woodhead: *Wavelengths effective in induction of malignant melanoma.* Proc. Natl. Acad. Sci (USA), **90,** 6666 (1993).

[3] S.R. Wood, M. Berwick, R.D. Ley, R.B. Walter, R.B. Setlow, G.S. Timmins: *UV causation of melanoma in Xiphophorus is dominated by melanin photosensitized oxidant production*, PNAS, **103**, 4111-4115 (2006)

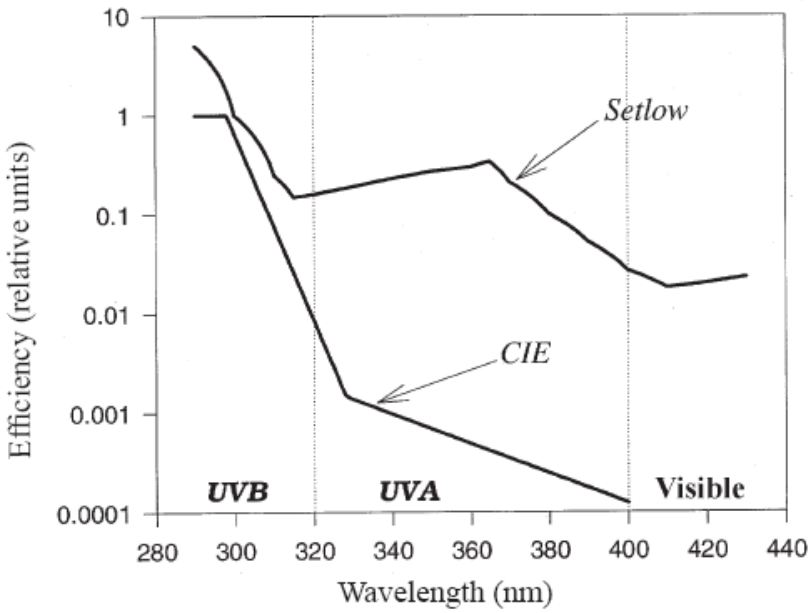

Figure 6.4*: Two important action spectra: the CIE-spectrum and the Setlow-spectrum. The CIE-spectrum is usually recommended for calculations of effective UV-doses. The shape of the spectrum is representative for formation of erythema. The Setlow-spectrum represents the formation of melanoma in the small fish, Xiphophorus.*

As explained above the efficiency spectrum $E(\lambda)$ is the product of the action spectrum $A(\lambda)$ and the solar spectrum $I(\lambda,t)$. We have calculated the efficiency spectrum based on the solar spectrum at midday (similar to the 1pm curve shown in Figure 6.3) and the CIE and Setlow action spectra. The results are shown in Figure 6.5. The dose rates at this specific time are found by integrating over all wavelengths from 290 nm to 430 nm.

It is very interesting to note that UVA, which is "independent" of ozone concentrations, more or less determine the entire UV-dose causing melanoma formation. The results also demonstrate the importance of using sunscreen with UVA protection in order to avoid skin cancer (malignant melanoma). In the last years sunscreen producers have been more aware of the possible negative effects of UVA.

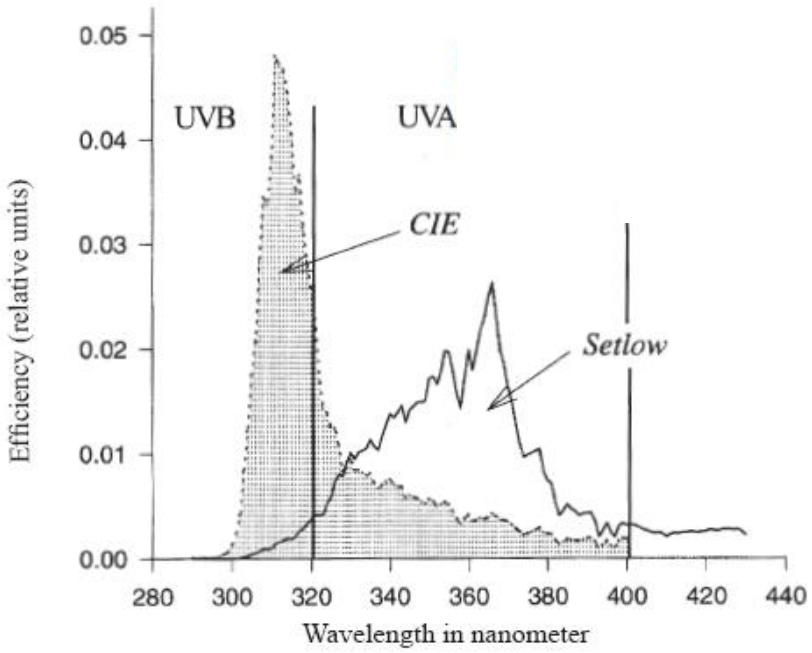

Figure 6.5: *Efficiency spectra based on CIE and Setlow action spectra. As explained in the text the efficiency spectra E(λ) is the product of the solar spectrum (which varies with time and place) and an action spectrum.*

6.3. Spatial and temporal UV-doses

The dose rate (integrated efficiency spectrum) will change during the day. Figure 6.6 shows an example of calculated UV dose rates at two places on the Northern Hemisphere, located at 40°N and 60°N. The calculations are made for two different dates under assumptions of a clear sky and "normal" ozone values. The CIE action spectrum has been used in the calculations.

As expected the dose rate is highest at low latitude due to a more intense sun. Around summer solstice (22nd of June) the dose rate at 40°N is 65-70% larger than the rate at 60°N. The difference increases in the course of the summer and reaches 100% 22nd of August. Figure 6.6 also demonstrates that the latitudinal differences are highest at noon and vanish in the morning and in the evening. The UV-dose for a full day is obtained by integrating the dose rate curves in Figure 6.6.

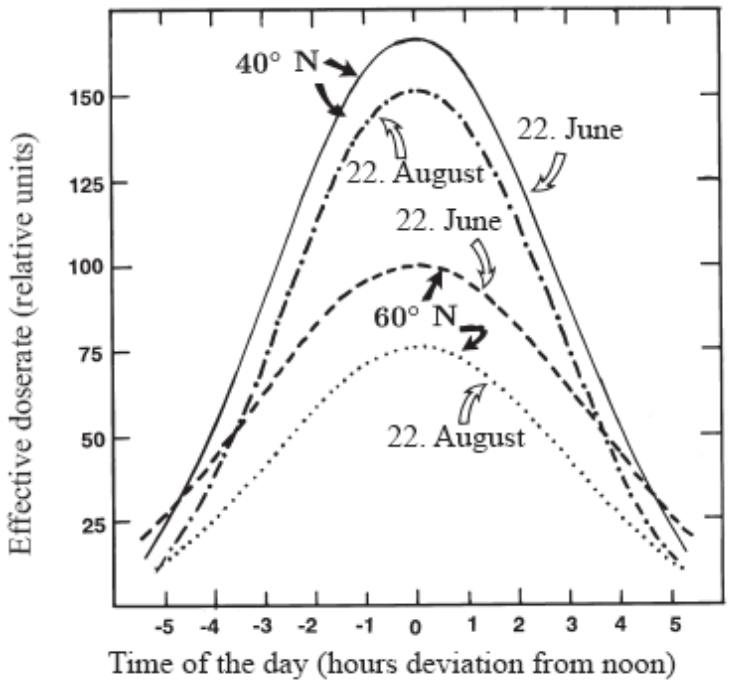

Figure 6.6: *Dose rate as a function of time of the day (based on CIE action spectrum and "clear sky" assumptions). Dotted and dashed curves represent 60°N. The ozone values used in the calculations are 350 DU in June and 300 DU in August for 60°N, whereas the values are 330 DU and 300 DU for June and August, respectively, at latitude 40°N.*

As we have seen in Chapter 4 the ozone layer varies throughout the year. Furthermore, the intensity of the sun varies. In order to calculate annual UV-doses we have divided the year into hours (8760 hours in a year) and assumed that the solar spectrum is constant within one hour. Based on this method we have calculated annual UV-dose for Oslo (60°N). In the calculations we have used "normal" seasonal ozone values (see Figure 2.5) and assumed a "clear sky". The total UV-dose for Oslo is set equal to 100.

We have made similar calculation for other latitudes, with ozone values equal to the latitudinal average values represented in Figure 2.3. The UV-doses for the different locations are calculated with a radiative transfer model. The results are presented in Figure 6.7 and show the UV-doses as a function of latitude. By moving from 60°N to the equator the UV-level increases by a factor 4.2 (using the CIE-spectrum) or about 2.1 using the Setlow spectrum. As can be seen from the figure the UV-dose is not a linear function of latitude, but between 60ºN and 20ºN the latitudinal UV variation is roughly 7% per degree (one degree latitude is 111 km). If the Setlow action spectrum is used the UV variation is only 3.5% per degree.

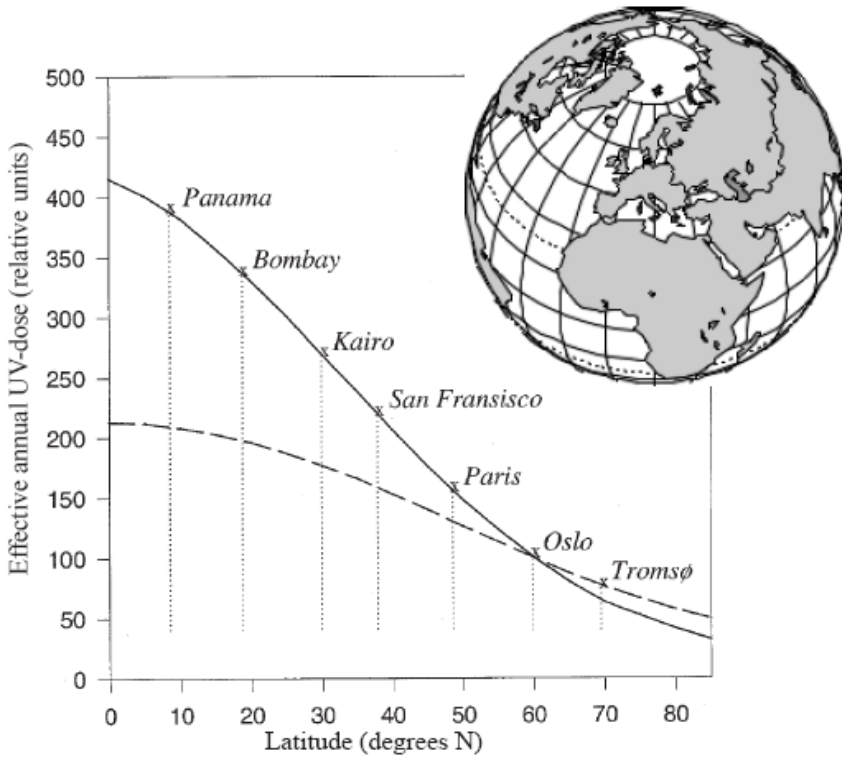

Figure 6.7*: Annual UV-doses as a function of latitude. The doses refer to sea levels and are given in relative units. A reference value of 100 is chosen for 60°N (Oslo). Two different action spectra are used in the calculations: The solid line refers to the CIE-spectrum, whereas the dashed line is obtained from the Setlow action spectrum.*

6.4. Correlation between ozone depletion and UV-doses

The ozone layer will efficiently absorb UV radiation from the sun. The question is: To what extent will a reduced ozone layer influence the UV-doses? In order to calculate the correlation between ozone depletion and increased UV-doses we have used a radiative transfer model and performed annual dose calculations under assumptions of a year-round ozone depletion of 5%, 10%, etc. In the calculations we have used both the CIE and Setlow action spectra. All the calculations are done for 60°N (i.e. Oslo).

The results from the calculations are visualized in Figure 6.8. Two important conclusions can be drawn from the figure:

1. By applying the CIE action spectrum it is evident that a small depletion of the ozone layer results in a similar increase in the UV-level. For example 5% ozone depletion will give roughly 5% increase in annual UV-dose. For 10% ozone depletion the UV increase is about 10% (slightly higher). A large ozone depletion of about 50% will increase the UV level at 60°N by about 120%, which is comparable to the UV level normally found at 38-40°N (i.e. San Fransisco).

2. The action spectrum plays a major role when the effect of ozone depletion is discussed. Figure 6.8 demonstrates large differences in the ozone-dependent dose calculations based on the CIE and Setlow action spectra. By applying the Setlow spectra 10% ozone depletion results in a UV-dose increase of less than 1%. This result implies that a depletion of the ozone layer will have a relatively small effect on the incidence of malignant melanoma.

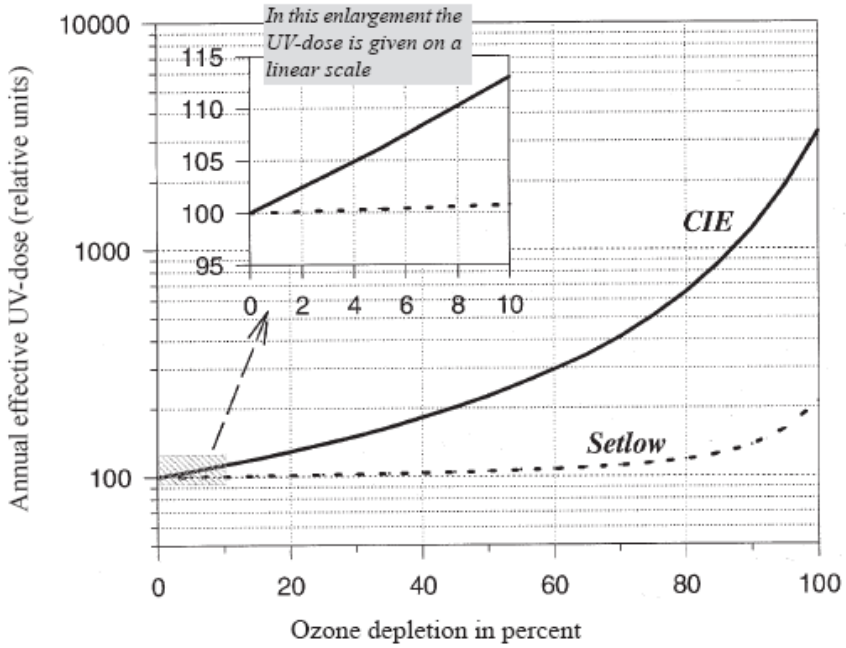

Figure 6.8: *Annual UV-doses at 60°N as a function of ozone depletion. The calculations are based on two different action spectra (CIE and Setlow) and the depletion is assumed constant throughout the year. The annual dose for a "normal" ozone layer (0% depletion) is set equal to 100. The depletions up to 10% are enlarged in the upper left corner of the figure.*

It should be pointed out that all the calculations presented above are based on a "clear sky". The cloud cover is of large importance for the UV-level and in order to make realistic calculations the clouds should be included.

6.4. UV index (UVI)

You have probably heard about the term **"UV index"** which is used to describe the strength of the sun and to inform the public about the health risk of sunbathing. But what is a UV index?

The UV index is a measure of the intensity of UV radiation, both UVA and UVB, and describes the expected risk of overexposure to the sun. The UV index is calculated from

the CIE action spectrum, meaning that the solar spectrum is weighted with the CIE action spectrum to obtain the dose rate. Next, the UV index is calculated by multiplying the CIE dose rate (given in W/m^2) by 40.

The UV index (also called UVI) predicts UV intensity levels on a scale of 1 to 11+, where 1 indicates a low risk of overexposure and 11+ signifies an extreme risk:

UV index	**Exposure level**
< 2	Low
3 to 5	Moderate
6 to 8	High
8 to 10	Very high
11+	Extreme

If the UV index is below 2 one can safely be outdoors without sun protection. For indices above 3, exposure to the sun can cause immediate effects such as sunburn. Protective clothing, sunglasses and sunscreen with high SPF (sun protection factor) should be used. If the UV index is very high one should seek shade and avoid the sun during midday.

Figure 6.9 shows UV indices measured in Oslo from January to mid August 2009. The values are obtained from the GUV instrument (see Chapter 3.2.3) at noon. The summer days with very low UV indices represent overcastted days.

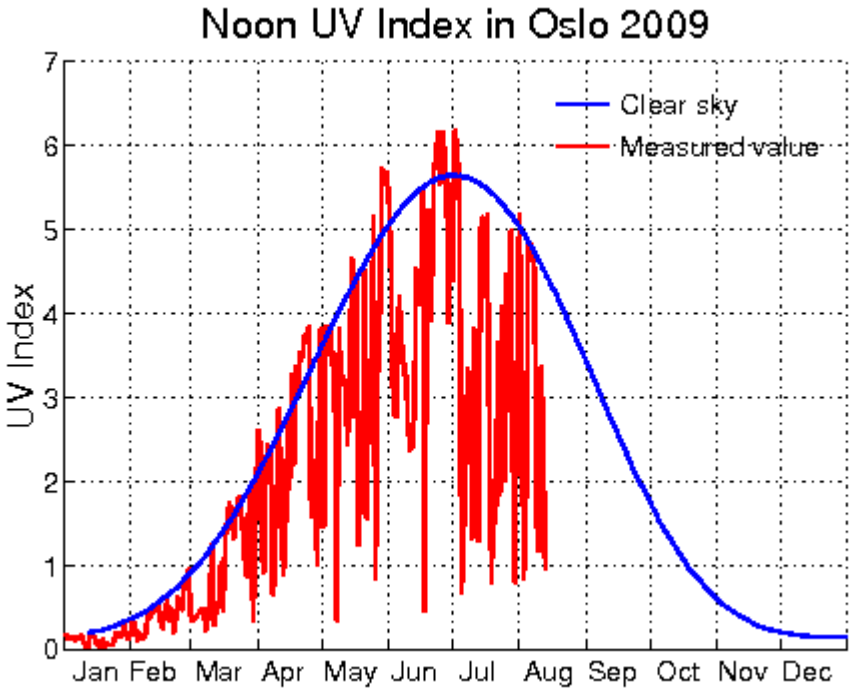

***Figure 6.9**: UV index from Oslo in 2009, measured at noon. The blue curve is modelled values with clear sky and "normal ozone", whereas the red curve represents measurements from the GUV instrument.*

Chapter 7

Radiative transfer in the atmosphere

This chapter gives a short introduction to radiative transfer in the atmosphere and applications of radiative transfer models (RTMs). An interesting and detailed description of the subject is given in the course FYS4630.

The aim of the calculations is to determine the intensity *I* as a general function of space and direction. We start by defining some fundamental variables.

7.1. Fundamental variables

Spectral intensity
Spectral intensity I_ν, also known as **radiance**, measures the energy flow within a solid angle dω around a certain direction **Ω** in the time interval *dt* and over a small increment of frequency. Further, we require that the radiation has passed through a surface element *dA* whose orientation is defined by its unit normal **n**. The angle between **n** and the direction of propagation **Ω** is denoted θ (i.e. **Ω**·**n** = cos θ). The energy *dE* per unit area, per unit solid angle, per unit frequency, and per unit time defines the spectral intensity:

$$I_\nu = \frac{d^4E}{\cos\theta dA dt d\omega d\nu}$$

The unit of spectral intensity (or radiance) is W m^{-2} sr^{-1} Hz^{-1}

Irradiance
The spectral irradiance F_ν, sometimes called **flux**, measures the net energy flow *dE* through a given surface, per unit area, per unit time, per unit frequency. Consider a surface with unit normal **n** parallel to the **Ω'** direction (i.e. **Ω'**·**n** = cos 0 =1). All radiant energy that crosses this surface contributes to the irradiance with 100% efficiency. Energy travelling orthogonal to **n** (parallel to the surface) never crosses the surface and does not contribute to the irradiance. The spectral flux (or irradiance) is expressed as

$$F_\nu = \frac{d^3E}{dA dt d\nu}$$

The unit of spectral flux (irradiance) is W m^{-2} Hz^{-1}

The relationship between flux and intensity is:

$$F_\nu = \int_{4\pi} I_\nu \cos\theta d\omega = \int_{\theta=0}^{\theta=\pi} \int_{\phi=0}^{\phi=2\pi} I_\nu \cos\theta \sin\phi d\theta d\phi$$

Optical depth and optical path

The extinction of radiation travelling a distance *ds* through a medium is: $dI=-k\cdot I\cdot ds$
The constant of proportionality, *k,* is called the extinction coefficient. It is convenient to introduce the dimensionless term:

Optical path: $$\tau_s = \int_0^s k(s')\cdot ds'$$

Another common term in atmospheric science is **optical depth** τ. It is the vertical component of the optical path τ_s, i.e. τ measures extinction between vertical levels. For historical reasons the optical depth in planetary atmospheres is defined as τ=0 at the top of the atmosphere and τ=τ* at the surface. It is convenient to measure the optical depth along the vertical direction downward from the top of the atmosphere (Z=∞):

Optical depth: $$\tau = \int_z^\infty k(z')\cdot dz' = \tau_s |u|$$

where $u=\cos\theta$ is the polar angle of the ray and $d\tau_s = -k\cdot u^{-1}\, dz$.
By convention we define k(∞)=0. When τ >1, the medium is said to be optically thick. The optical depth is a mixture of extinction due to scattering and absorption. The scattering and absorption coefficients are named σ and α, respectively. Thus, $\tau=\tau_\sigma+\tau_\alpha$

7.2. Radiative transfer equation

The general equation for radiative transfer in a medium with multiple scattering and absorption is:

$$\frac{dI_\nu}{d\tau_s} = -I_\nu + [-a(\nu)\overline{B}_\nu(T) + \frac{a(\nu)}{4\pi}\int_{4\pi} d\omega\cdot p(\hat{\Omega}',\hat{\Omega})\cdot I_\nu(\hat{\Omega}')$$

$a(\nu)$ = single scattering albedo (ratio of scattering to total extinction, i.e. $\sigma(\nu)/k(\nu)$)
B_ν = Planck function (intensity of emitted radiation with frequency ν)
$p(\Omega', \Omega)$ = Phase function (the probability that radiation with incoming direction Ω' will be scattered in direction Ω)

In order to solve the radiative transfer equation it is assumed that the atmosphere is divided into *n* parallel layers, where each layer has a homogeneous composition. Detailed descriptions of how to solve the equation are presented in FYS4630

7.3. Application of radiative transfer models

A radiative transfer model can be used for many purposes. Some of the applications have previously been mentioned in this compendium. Presently we use the radiative transfer models (RTM) at Blindern and NILU for the following purposes:

- To analyse data from ground based instruments and to develop algorithms for satellite retrievals.
- To develop software for ozone filter instruments
- To calculate UV-levels (intensity, UV-doses, UV indices) in the past, present and future.
- To study the impact of climate changes, i.e. how changes in atmospheric compositions, surface albedo and temperatures influence the radiative balance
- To improve parameterisations in climate models

Exercises

Exercise 1

a) Use the ideal gas law to derive the expression for air pressure as a function of altitude: $p(z)=p(0)\exp(-z/H)$.
b) What is the scale height at temperature 273K?
c) Find the tropopause and stratopause pressures at temperature 273K.

Exercise 2

Calculate the average solar energy reaching the ground. Assume that the solar constant is 1367 W/m^2 and the albedo is 0.3.

Exercise 3

a) Derive the general expression for direct sun ozone measurements from a single wavelength pair.
b) The Dobson instrument is used for total ozone measurements in Oslo 7th June at 11.30 GMT (Z=37.2). The measurements are based on C direct sun observations. An instrumental optical slab is adjusted until $I(\lambda)=I(\lambda')$, representing a dial reading of R=65.2. How thick is the ozone layer (in DU)?

Useful information:

- Absorption coefficients for the C-pair: $\alpha-\alpha'=0.833$ $(atm\ cm)^{-1}$
- Rayleigh scattering coefficient: $\beta(\lambda)=k\cdot\lambda^{-4}$, where $k=4.27656\cdot10^9$ (nm^4/atm).
- The N-values are defined as $N=100(\ln(I'/I)-\ln(I'_0/I_0))$. The following relationship between instrumental readings R and N-values is established for the instrument: $N=0.95\cdot R-13.5$

Exercise 4

Assume that the ozone molecules in the stratosphere are formed with a rate of $5\cdot10^{31}$ s^{-1}. How many days will it take to produce an ozone layer of 320 DU if all destructive processes are ignored?
(Earth radius $R=6.38\cdot10^6$m, Avogadros number $A=6.02\cdot10^{23}$, volume of one mole gas $M=22.4\cdot10^{-3}m^3$).

Exercise 5

On a sunny day the solar spectrum in the UV region is roughly described by the linear function:
$I(\lambda) = 0.0069\lambda - 2.0558$ $(W/m^2\ nm^{-1})$ for $\lambda > 300$ nm
$I(\lambda) = 0$ for $\lambda < 300$ nm

What is the UV index? (It is enough to set up the equations, alternatively the integral $\int x\cdot exp(x)dx$ can be solved from a computer program where $\Delta x=1$nm).

References

Dahlback, A., Measurements of biologically effective UV doses, total ozone abundances, and cloud effects with multichannel, moderate bandwidth filter instruments, Appl. Opt., Vol. 35., No.33, 6514-6521, 1996

Henriksen, T., and Svendby, T., Ozonlag, UV-stråling og helse, Department of Physics, University of Oslo. ISBN 82-992073-9-8, 176 pages, 1997

IPCC, Climate Change 2007: The Scientific Basis. Contribution of Working Group I to the Fourth Assessment Report of the Intergovernmental Panel on Climate Change, 2007

Seinfeld, J. H., and S. N. Pandis, Atmospheric chemistry and physics, New York: John Wiley &Sons, 1998

Stordal, F., and Ø. Hov, Luftforurensninger: Sur nedbør, ozon, drivhuseffekt, Oslo, Universitetsforlaget, 1993